Shank2 및 *Snf7-3* 유전자 결손 생쥐를 이용한 신경발달장애의 행동학적, 분자생물학적 연구

Behavioral and molecular studies on the neurodevelopmental disorders using *Shank2* and *Snf7-3* knock out mice

2019년 2월

서울대학교 대학원

자연과학대학 생명과학부

김 효 필

Shank2 및 *Snf7-3* 유전자 결손 생쥐를 이용한 신경발달장애의 행동학적, 분자생물학적 연구

Behavioral and molecular studies on the neurodevelopmental disorders using *Shank2* and *Snf7-3* knock out mice

지도교수 강 봉 균

이 논문을 이학박사 학위논문으로 제출함
2019년 01월

서울대학교 대학원
생명과학부
김 효 필

김효필의 이학박사 학위논문을 인준함
2018년 12월

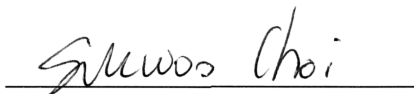| 위 원 장	희 1상우	(인)
부 위 원 장	강 봉 균	(인)
위 원	한 진 희	(인)
위 원	윤 태 영	(인)
위 원	이 진 아	(인)

Behavioral and molecular studies on the neurodevelopmental disorders using *Shank2* and *Snf7-3* knock out mice

Advisor: Bong-Kiun Kaang

A dissertation submitted in partial fulfillment of the requirement for the degree of
DOCTOR OF PHILOSOPHY

To the Faculty of the
School of Biological Sciences
at
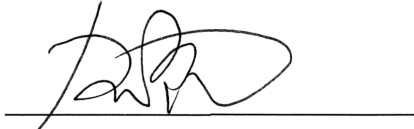Seoul National University
by
Hyopil Kim
January 2019

Thesis committee:

Sukwoo Choi
Committee Chairman

Bong-Kiun Kaang
Vice Chairman

Tae-Young Yoon
Member

Jin-A Lee
Member

Jin-Hee Han
Member

ABSTRACT

Behavioral and molecular studies on the neurodevelopmental disorders using *Shank2* and *Snf7-3* knock out mice

Hyopil Kim

School of Biological Sciences

The Graduate School

Seoul National University

Neurodevelopmental disorders are defined as a group of conditions caused by developmental deficits with onset in the relatively early period of lifetime, which produce cognitive and behavioral abnormalities including learning, memory, locomotion, attention and social functions according to the fifth edition of Diagnostic and Statistical Manual of Mental Disorders (DSM-5). They are classified into disorders such as intellectual disabilities, autism spectrum disorder (ASD), attention deficit hyperactivity disorder (ADHD), obsessive compulsive disorders and tic disorders by specific behavioral and mental symptoms, and in many cases patients of neurodevelopmental disorders share some symptoms. However, the causes and physiological mechanisms of each disorder is not well understood yet, and even in one category of disorder, it seems that various distinct mechanisms are implicated in it.

Among the neurodevelopmental disorders, ASD is characterized by deficits of sociability, social communication, repetitive behaviors and restricted interests. Because of its high prevalence, genetic analyses of ASD patients have been done worldwide and these studies indicate that many synaptic genes including SH3 and multiple ankyrin repeat domains protein 2 (*SHANK2*) are involved in ASD. Concomitantly with these studies, two *Shank2* knock out mice line with deletion of exon 6 and 7 (*Shank2* KO e67) and with deletion of exon 7 (*Shank2* KO e7) were characterized

as autistic behaviors. However, when I analyzed the transcriptome of the two lines, expression of *Gabra2* gene, encoding γ-aminobutyric acid (GABA) A receptor subunit α2 (GABAAα2) and inhibitory neurotransmission were reduced only in *Shank2* KO e67. The excitatory neurotransmission was normal, so the excitatory and inhibitory balance (E/I balance) was impaired. Restoring this inhibitory neurotransmission could rescue spatial memory deficits of *Shank2* KO e67 mice, while it did not affect the spatial memory deficits of *Shank2* KO e7 mice.

In addition to the work, I investigated if the endo-lysosomal pathway is involved in the neurodevelopmental processes. Interestingly my colleague found that when the expression of Snf7-3 protein, a component of endosomal sorting complexes required for transport III (ESCRT-III), was reduced in developing neuron culture, the dendrite outgrowth was exaggerated. To examine this phenotype is involved with the symptoms of neurodevelopmental disorders, I generated conventional and conditional KO mice of *Snf7-3*, and the mice displayed hyperactivity which is the main symptom of ADHD. Furthermore, in the conditional KO mice, object location memory was also impaired. In addition, since the E/I balance of neurotransmission is often disturbed in the model mice of neurodevelopmental disorders, I assessed this possibility and found that the frequency of spontaneous excitatory neurotransmission was elevated in the KO mice of hippocampus.

....

CONTENTS

Chapter I. Introduction

Chapter II. Distinct mechanisms accounted for behavioral deficits of two *Shank2* KO lines

Chapter III. Role of *Snf7-3* in neurodevelopmental disorders regulating the dendritic developmental processes

LIST OF FIGURES

CHAPTER I

INTRODUCTION

BACKGROUND

Causes of neurodevelopmental disorders

Neurodevelopmental disorders are defined as a group of pathological conditions including various deficits in intellectual abilities, attention, locomotion and social functions with onset in the relatively early period of lifetime. They are not convergent to one disorder and even in same disorder, the symptoms and causes are quite different. Consistently with the complex property of neurodevelopmental disorders, various environmental and genetic factors have been identified implicated in the disorders.

Environmental factors include prenatal exposure to valproic acids, gut microbiota and maternal obesity, increasing the incidence of neurodevelopmental disorders, especially ASD (Buffington et al., 2016; Li et al., 2017a; Schneider and Przewłocki, 2005). Genetic studies have identified hundreds genes related with a lot of biological processes, such as synaptic scaffolding proteins, neurotransmitter receptors, adherent molecules, cytoskeletal proteins and signaling molecules. Although it is difficult to find out general mechanism for neurodevelopmental disorders, it seems that the factors cause developmental delays and abnormal brain connectivity. For example, lots of genes are found to be interact with signaling proteins of Rho GTPases pathways which is critical for synapse development (Govek et al., 2005). In addition, mutations in genes involved in regulation of mRNA translation of synaptic proteins are also found to be related with neurodevelopmental disorders, including fragile X mental retardation protein (FMRP), tuberous sclerosis protein 1/2 and eukaryotic translation initiation factor 4E (eiF4E) (Gkogkas et al., 2013; Schneider and Przewłocki, 2005; The Dutch-Belgian Fragile et al., 1994). Mutations in the genes cause dysregulation of protein synthesis, altering synaptic density and neurotransmission properties.

E/I balance

Fine tuning of activation or inhibition of a specific population of neurons is important for the adequate development and function of brain, and a neuron can regulate the activity of another neuron by excitatory or inhibitory neurotransmission. The most well-known excitatory and inhibitory neurotransmitter is glutamate and GABA respectively. There are two major ionotropic glutamate receptors, α-amino-3-hydroxy-5-methyl-4-isoxazolepropionic acid (Gkogkas et al.) receptor and N-methyl-D-aspartate (NMDA) receptor, that can activate a neuron after binding glutamate by generating positive sodium or calcium ion influx. Similarly, GABA can inhibit a neuron with GABA receptors (GABA-R) which are divided into GABAA and GABAB receptors, by generating negative chloride influx. Thus, if there are alterations in the neurotransmitter release and the number or conductance of the receptors, the E/I balance can be disturbed and this condition possibly result in abnormal pathophysiological conditions. Indeed, many mouse models of neurodevelopmental disorders such as *Shank2* KO and *Cntnap2* KO mice have disturbed E/I balance, and social and cognitive functions can be regulated by manipulating E/I balance in specific brain areas (Lee et al., 2017; Peñagarikano et al., 2011; Schmeisser et al., 2012; Won et al., 2012; Yizhar et al., 2011).

Hyperactivity and neurodevelopmental disorders

Hyperactivity is a main symptom of ADHD which is a major neurodevelopmental disorder. The term of hyperactivity means exaggerated motions and locomotion in both vertical and horizontal directions. Although the hyperactivity itself is not a main diagnosis criteria of the other neurodevelopmental disorders, in many cases, patients and animal models of neurodevelopmental disorders, including autism display the hyperactivity. For example, autistic mouse models such as *Shank2* KO, *Cntnap2* KO and *Scn1a* +/-, are found to be hyperactive (Han et al., 2012; Peñagarikano et al., 2011; Schmeisser et al., 2012; Won et al., 2012). In addition, patients of autism or tic disorders are characterized by repetitive behaviors which are regulated by the cortico-striatal circuit that also regulates locomotion (Kim et al., 2016).

RNA sequencing

 Finding molecular targets of specific biological processes is very important to understand the molecular mechanisms of the processes. There are many methods to test if a candidate molecule is a really important molecule, but it is not easy to set the candidate molecules. Moreover, nowadays, a pathological condition is thought to be resulted from dynamic alterations in a molecular profile rather than from alteration in one molecule. For the reasons, RNA sequencing is a widely used technique that provides a RNA transcriptome profile, and by comparing the transcriptome, we can get a clue for actual important molecules. For that purpose, mRNA is extracted from a sample and fragmented, and copied into cDNA. This cDNA library is sequenced by short-read sequencing. Each reads are aligned to a reference genome and quantitative analysis about gene expression can be made from the data.

Three-chamber test

  Three-chamber test is a behavioral test which addresses sociability and social recognition (Figure 1A). The test has been widely used to investigate social behaviors of animal models since when it was developed by Jacqueline N. Crawley (Moy et al., 2004). The test is composed of two phases. At the first phase, a mouse is placed in a center chamber of sequential three chambers. In the two chambers of outside, a social target, stranger mouse, or a non-social target, such as a little block, is presented in a wired cup respectively. A subject mouse spends time exploring the targets, and normal mice usually display much higher exploration to the social target. If a mouse has a problem in sociability, it would not spend much time with the stranger mouse. At the second phase, the non-social target is replaced with new stranger mouse and in this phase, normal mice spend more time with a novel stranger, because they have instinct to explore novel social target. If a mouse has poor social recognition ability, the mouse cannot distinguish the novel stranger from the prior one. Autistic mice usually display abnormal sociability or social recognition in the test (Han et al., 2012; Peñagarikano et al., 2011; Schmeisser et al., 2012; Won et al., 2012).

Morris-water maze

  Morris-water maze is developed by Richard G. Morris in 1981 as a test for spatial memory, and

many reports have shown that the spatial memory is dependent on proper hippocampal function in the task (Morris et al., 1982; Vorhees and Williams, 2006). In Morris-water maze, a platform (mouse cannot see the platform because the plat form is hidden under the surface of opaque water) is prepared in a water pool and specific spatial cues are presented around the pool. Then a mouse is placed in the pool and the mouse try to escape from the pool, since mice do not like being soaked in water and mice feel more comfortable on the hard platform. In the training session, mice were guided to find the platform so they learn the location of the platform based on the spatial cues. After this training sessions, a probe test is performed in which mouse is exposed to the pool again without platform, and the time spent near the platform position is assessed (Figure 1B).
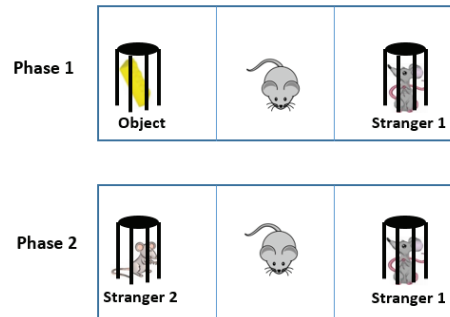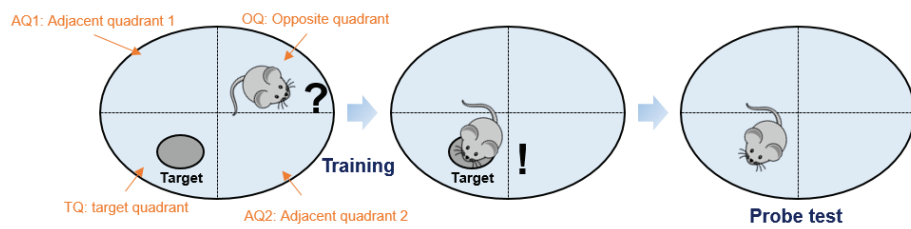
Figure 1. Representative images of three-chamber test and Morris-water maze

(A) Representative images of three-chamber test

(B) Representative images of Morris-water maze

PURPOSE OF THIS STUDY

1. Distinct mechanisms accounted for behavioral deficits of two *Shank2* KO lines

Despite to the high prevalence of ASD, there is no general effective treatment for ASD and lots of researchers are still trying to understand the mechanisms of ASD and develop effective treatments for the disorder. However, the heterogeneity of ASD makes it difficult to study and treat the disorder.

For the purpose of studying the neuronal and molecular mechanisms of ASD, genetic analyses of ASD patients have been done globally. Interestingly, these studies indicated that many synaptic genes are involved with ASD including *SCN1A*, *CNTNAP2* and *NRXN1A* (Kim et al., 2008; Strauss et al., 2006; Weiss et al., 2003). Among the synaptic genes involved in ASD, genes encoding SH3-Ankirin and proline rich synaptic associated protein, Shank, are strongly associated with neuropsychiatric disorders (Guilmatre et al., 2014). Furthermore, it was found that copy number variations in *SHANK2* gene is involved with ASD and mental retardation (Berkel et al., 2010). Based on this, a group of researchers, investigated if *Shank2* deleted mice display autistic behaviors and if so, what the underlining mechanism of the behaviors is.

For that purpose, our laboratory investigated autistic behaviors of *Shank2* KO e67 and showed that the KO mice have social impairment, repetitive jumping behavior and intellectual disabilities. Furthermore, the neurotransmission through N-methyl-D-aspartate receptors (NMDA-R) is weakened in the mouse and enhancing the function of NMDA-R ameliorated the social deficit of the *Shank2* KO e67 mice (Won et al., 2012). Consistently with the findings, another group reported that another *Shank2* KO mouse, *Shank2* KO e7 mouse, also displays autistic like phenotypes including social deficits. However, interestingly, the NMDA-R function was not weakened in the KO mice, rather enhanced (Schmeisser et al., 2012). Thus, I hypothesized that their behaviors may be resulted from

different molecular mechanisms even though the behavioral patterns are quite similar.

Researchers made ASD model mice based on the candidates, and they studied physiological and molecular characteristics of the models. However, the phenotypes of the models were not convergent even if they have similar deficits related with ASD (Kim et al., 2016). Since the causes of ASD are not well known, and the symptoms of ASD are quite variable, I do not think that one golden solution exists for ASD. Specific molecular mechanisms underlying a specific behavioral deficit should be studied and treatment also be done according to the mechanisms. Moreover, it is possible that different molecular mechanisms underpin same behavioral deficits. Therefore, to understand the mechanisms of ASD we need non-biased studies, and should know detailed causes of a specific phenotype to treat ASD efficiently.

The goal of this study is to compare molecular and physiological profiles of the two *Shank2* KO lines, and find out which mechanism is accounted for each behavioral deficit of the lines. In addition, the final goal is to rescue the deficits based on the mechanism.

2. Role of *Snf7-3* in regulating the neurodevelopmental processes

Snf7-3 is a protein which is a member of Snf7 family, and also known as chromatin-modifying protein/charged multivesicular body protein 4C (Chmp4C). Snf7 proteins are components of endosomal sorting complex required for transport III (ESCRT-III), and the complex is involved in the endo-lysosomal pathway, regulating multivesicular body (MVB) formation (Schuh and Audhya, 2014). ESCRT-III is composed of Vps20, Snf7, Vps24 and Vps2 and they form a spiral structure in membrane of endosome or plasma membrane, so influencing MVB formation, cytokinesis and virus budding (Henne et al., 2011).

In addition to that, a drosophila homolog of Snf7, Shrub, is involved in the pruning of dendrites in developing neurons, regulating the morphology of the neurons (Loncle et al., 2015; Sweeney et al., 2006). However, it is not well-known that if Snf7 or ESCRT-III has a role in neurodevelopmental processes in mouse. Mouse has two paralogues of Snf7, Snf7-2 and Snf7-3, and my colleague showed that in primary neuron culture, dendritic development was

decreased when she reduced the expression of *Snf7-2* (Lee et al., 2007). Interestingly, according to her, reducing the expression of *Snf7-3* caused the opposite phenomenon increasing the dendritic development. Furthermore, *Snf7-3* was most highly expressed on DIV6 in mouse primary culture, when the development of culture neurons is vigorous, including dendrite outgrowth and maturation. Thus I became interested in the protein and thought that it might be implicated in neurodevelopmental disorders. Supporting this, a genetic study of human patients indicated that (SNPs) in *CHMP7*, a homologue of *SNF7*, may be involved in ADHD (Neale et al., 2010).

Therefore, I generated *Snf7-3* KO mice and addressed if the depletion of *Snf7-3* would affect the regulation of dendrite complexity in vivo. In addition, I examined if the *Snf7-3* KO mice display some physiological and behavioral features of neurodevelopmental disorders.

CHAPTER II

Distinct mechanisms accounted for behavioral deficits of

two *Shank2* KO lines

INTRODUCTION

ASD is diagnosed based on social deficits, communication deficits, stereotypic behaviors and restricted interests according to DSM-5. In addition to the primary symptoms, lots of ASD patients have intellectual disabilities and 25–75% of them have learning and memory problems (O'Brien and Pearson, 2004). Furthermore, consistently with the term of 'Spectrum', the patients show various range of cognitive deficits and the severity of the symptom is also divergent. For instance, some patients are hyperactive, while others are hypoactive. Some patients show microencephaly, while others show megalencephaly (Fombonne et al., 1999).

For the last decades, the number of ASD patients have been increased dramatically and recent surveys said that the prevalence of ASD is 1 in 42 children in United States and 1 in 38 children in South Korea (Kim et al., 2011; Zablotsky et al., 2015). As the most frequently occurring neurodevelopmental disorder, it demands tremendous social payment for treating the patients. However, despite the high prevalence of ASD, there is no effective treatment for the disorder. Just risperidone and aripiprazole are approved by FDA for treating ASD patient to reduce irritability, while they are not that effective for main symptoms of ASD.

ASD is thought to be caused by both genetic and environmental factors. Nowadays, some environmental factors implicated in ASD have been uncovered, such as administration of valproic acid during pregnancy or alteration in the balance of the gut microbiome (Christensen et al., 2013; Li et al., 2017a). On the other hand, ASD is highly heritable disorder and a lot of studies have discovered ASD associated genes by genome analyses. About 20% of ASD cases are involved with genetic and epigenetic variations including alterations in chromosomal structures, copy number variations and mutations in coding sequences (Leblond et al., 2014). According to Simons Foundation Autism Research Initiative, SFARI, over a thousand of ASD risk genes are scored and estimated.

Among them, genes encoding synaptic proteins are one of the most highlighted gene group, including ion channels, adhesion molecules and scaffolding proteins, such as *SCN1A*, *CNTNAP2*

and *NRXN1A* (Kim et al., 2008; Strauss et al., 2006; Weiss et al., 2003). Based on the genetic studies of human patients, dozens of animal models were generated by mimic the mutations of the candidate genes, and some animals actually displayed social deficits and repetitive behaviors which are main symptoms of ASD (Etherton et al., 2009; Han et al., 2012; Peñagarikano et al., 2011).

SHANK encoding SH3 and multiple ankyrin repeat domains protein, Shank, is one of the genes which is implicated in ASD. Shank protein is a major synaptic scaffolding protein in excitatory synaptic spines, make a network between glutamate receptors such as NMDA-R and mGluR, and actin structures. Mammalian *SHANK* family of genes is composed of *SHANK1*, *SHANK2* and *SHANK3*. All the *SHANK* genes are dynamically involved in neuropsychiatric diseases and ASDs. About 1~2 % of patients with ASD or intellectual disabilities patients have mutations in the *SHANK* genes (Leblond et al., 2014).

Especially, it was found that copy number variations in *SHANK2* gene is involved with ASDs and mental retardation (Berkel et al., 2010). Based on this, a group of researchers including our lab, investigated if *Shank2* deleted mice display autistic behaviors and if so, what the underlining mechanism of the behaviors is. For that purpose, we investigated autistic behaviors of *Shank2* KO e6-7 and showed that the KO mice have social impairment, repetitive jumping behavior and intellectual disabilities. Furthermore, the neurotransmission through N-methyl-D-aspartate receptors (NMDA-R) is weakened in the mouse and enhancing the function of NMDA-R ameliorated the social deficit of the *Shank2* KO e6-7 mice (Won et al., 2012). Consistently with the findings, another group reported that another *Shank2* KO mouse, *Shank2* KO e7 mouse, also displays autistic like phenotypes including social deficits. However, the NMDA-R function was not weakened in the KO mice, rather enhanced (Schmeisser et al., 2012).

This implies that the two KO lines may have different molecular mechanisms for their behavioral and physiological symptoms, and different treatment will work. Studying this differences would help to understand various mechanisms for autistic behaviors.

To compare the molecular differences of the two KO lines I conducted unbiased RNA sequencing in the hippocampus and analyzed the transcriptomes of them. Interestingly, I found that the expression of *Gabra2* gene which encoding GABAAα2, was reduced in *Shank2* e67 KO

mice while it was intact in *Shank2* KO e7 mice.

GABAA receptors are ligand-gated chloride channels and consist of two α subunits, two β subunits and one γ subunit. The subcellular localization is dependent on their composition and GABAA receptors containing α1–3 are mainly synaptic, while receptors containing α4–6 subunits are mainly extrasynaptic (Belelli et al., 2009). Especially GABAAα2 is important for regulating neuronal activities and implicated in emotional processes such as anxiety and depression, and the CNS development (Dixon et al., 2008; Gonzalez-Nunez, 2015).

In relation with ASD, alterations of GABAergic signaling or disturbed E/I balance is commonly found in the neurodevelopmental disorders (Braat and Kooy, 2015; Han et al., 2014; Han et al., 2012; Robertson et al., 2016). Several mouse models harboring ASD-associated mutations display altered ratio of E/I ratio (Cui et al., 2008; Gkogkas et al., 2013; Han et al., 2012; Houbaert et al., 2013; Lee et al., 2014; Tabuchi et al., 2007). In addition, copy-number variations (CNVs) in chromosome 15q11–13 which includes genes encoding GABAA receptor subunits, have been found in patients of a type of ASD, Prader-Willi/Angelman syndrome. (Hogart et al., 2007; Scoles et al., 2011). Furthermore, it was found that GABA receptor subunits are less expressed in ASD patients by post-mortem studies (Fatemi et al., 2014; Oblak et al., 2011).

Thus I hypothesized that this difference might be accounted for the differences of the *Shank2* KO lines. Consistently with the reduced expression of *Gabra2*, GABA-R mediated synaptic transmission was reduced in e6-7 KO, while the excitatory AMPA receptor (AMPA-R) mediated synaptic transmission was normal, so alternating the E/I ratio. Then I applied an agonist of GABAA receptor including the alpha 2 subunit, L838,417, to see if it can rescue some behavioral deficits of the *Shank2* e6-7 KO mice. Treatment of L838,417 did not affect the social impairment of the two *Shank2* KO mice. However, the treatment of L838,417 reverses spatial memory deficits in *Shank2* e6-7 KO mice, while it had no effects in *Shank2* e7 KO mice. These findings would be attributed to understanding the heterogeneity of ASD and developing effective treatments for each patient.

EXPERIMENTAL PROCEDURES

Animals

I used two *Shank2* KO mouse lines, *Shank2* KO e67 and *Shank2* KO e7, for following experiments. They were targeted and deleted exon6 and exon7, or only exon7 respectively (Figure 2). Each line had been backcrossed to C57Bl/6N and C57Bl/6J respectively. To generate homogeneous KO mice and WT littermates, I crossed heterogeneous male with heterogeneous female mice. For the RNA sequencing, western blot and electrophysiological experiments, 4 to 5 weeks old male mice were used and for the behavioral experiments, 8 to 15 weeks old male mice were used.

Food and water were provided *ad libitum* and all the mice were kept on a 12 h light/dark cycle. All the experimental procedures were done during the light phase of the cycle. The Institutional Animal Care and Use Committee of Seoul National University approved the animal care and experiments.

(Adapted from Won et al., 2012)

(Adapted from Schmeisser et al., 2012)
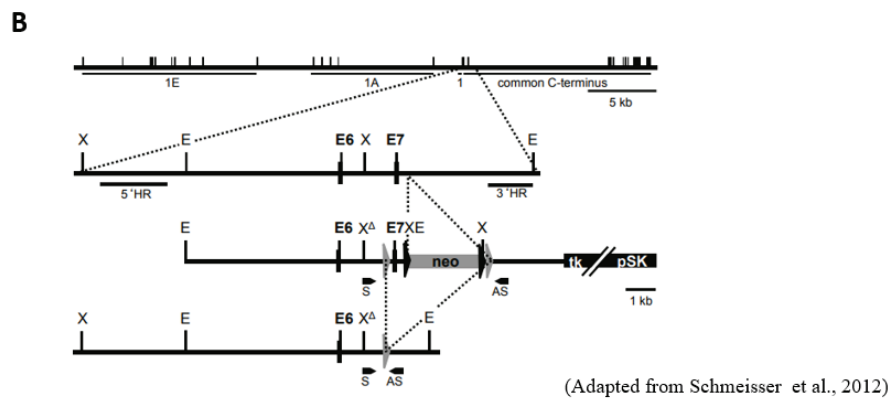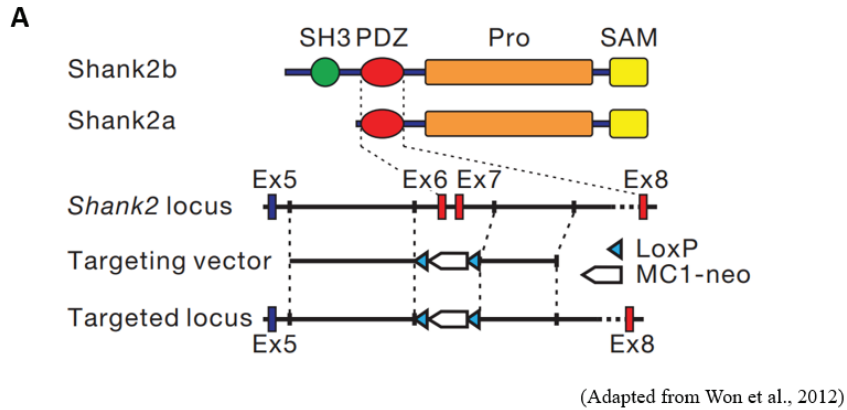
Figure 2. Strategies to delete *Shank2* by targeting exon 6 and 7 or only exon 7

(A) KO strategy to delete *Shank2* by targeting exon 6 and 7

(B) KO strategy to delete *Shank2* by targeting exon 7

RNA sequencing

After anesthetization with isoflurane, hippocampi of *Shank2* KO e67 or *Shank2* KO e7 mice with their respective littermate WT mice was extracted. To make RNA libraries, the hippocampus was grinded and total RNA was separated by TRIZOL (Invitrogen). 5 μg of poly-A mRNA was processed by Illumina Truseq RNA Sample Prep Kit with poly-T oligo-attached magnetic beads. To make cDNA libraries, reverse transcription was performed using Superscript II reverse transcriptase (Life Technologies). The adaptor-ligated libraries were separated in gel electrophoresis and extracted using QIAquick gel extraction kit (Qiagen). These libraries were sequenced on Illumina HiSeq 2500 (NICEM, Seoul National University) in the paired-end sequencing mode (2 × 101 bp reads), and these raw reads were mapped onto the mouse genome reference mm10 using GSNAP (version 2013-11-27). Uniquely and properly mapped read pairs were used for further analysis.

Gene expression level was calculated based on the RPKM (reads per kilobase of exon per million mapped reads) measure. To identify differentially expressed genes (DEGs) between the WT and KO groups, cuffdiff module in the Cufflinks package (version v2.1.1) was used and in this analysis DEGs were defined as those with changes of at least 1.5-fold between samples at a false discovery rate of 10%. Finally, PANTHER (Protein ANalysis THrough Evolutionary Relationships) Tools (http://www.pantherdb.org/) and GO term enrichment analysis were used to divide the DEGs into biological and functional protein classes.

Quantitative real time-PCR (qRT-PCR)

cDNA samples were generated from RNA samples used for RNA sequencing. qRT-PCR was performed using ExTaqII SYBR Green Master Mix (Takara) in ABI7300 (Applied Biosystems) system. Primer sequences for each gene are listed below.

Shank1 5' CCGCTACAAGACCCGAGTCTA 3' 5' CCTGAATCTGAGTCGTGGTAGTT 3'
Shank3 5' CCGGACCTGCAACAAACGA 3' 5' GCGCGTCTTGAAGGCTATGAT 3'
Gria1 5' GTCCGCCCTGAGAAATCCAG 3' 5' CTCGCCCTTGTCGTACCAC 3'

Gria2 5' TTCTCCTGTTTTATGGGGACTGA 3' 5' CTACCCGAAATGCACTGTATTCT 3'

Gria3 5' ACCATCAGCATAGGTGGACTT 3' 5' ACGTGGTAGTTCAAATGGAAGG 3'

Grin1 5' TGGCCGTGTGGAATTCAATG 3' 5' TTGTGGGCTTGACATACACG 3'

Grin2a 5' GACATCCACGTTCTTCCAGTT 3' 5' GGCGTCCTCAAAAGAGGTGT 3'

Grin2b 5' GCCATGAACGAGACTGACCC 3' 5' GCTTCCTGGTCCGTGTCATC 3'

Dlg4 5' ACCAGAAGAGTATAGCCGATTCG 3' 5' GGTCTTGTCGTAGTCAAACAGG 3'

Dlgap1 5' AAACCGATGTCTGTCTATTGGGA 3' 5' GGGCCAGGACACGAATTGT 3'

Grm1 5' TGGAACAGAGCATTGAGTTCATC 3' 5' CAATAGGCTTCTTAGTCCTGCC 3'

Grm5 5' CCCAGCACAAGTCGGAAATAG 3' 5' TGTCTGGTTGGGGTTCTCCTT 3'

Gabra2 5' CCAAGTGTCATTCTGGCTGA 3' 5' GCCCATCCTCTTTTTGTGAA 3'

Cycling conditions were 95 °C for 30 s, followed by 40 cycles of 95 °C for 5 s and 60 °C for 31 s. GAPDH was used as an internal control for each gene.

L838,417 preparation

L838,417 (Sigma, L9169) was dissolved in DMSO at 10 mg/ml and aliquots of L838,417 was stored at −20 °C. To administrate L838,417 in the behavioral experiments, 10 mg/ml of L838,417 was diluted in saline to a final concentration of 0.02 mg/ml. DMSO diluted in saline at a concentration of 0.2% was used as a vehicle. 0.02 mg/ml of L838,417 and 0.2% DMSO were also stored at −20 °C and thawed immediately before to use. 5 ml/kg (0.1 mg/kg) of L838,417 or vehicle was injected intraperitoneally for the behavioral experiments. Drug injection was randomized by other experimenters who did not perform behavior experiments.

Behavioral Tests

Elevated zero maze (EZM) test

A round-shaped (inner diameter: 50 cm, outer diameter: 60 cm) maze which is made of white Plexiglass and elevated 40 cm from the floor, was used. The maze was composed of 4 arms, 2 of open arms and 2 of closed arms with 20 cm walls on both sides. A mouse was placed on the center

of one of closed arm of the maze, and the movement of the mouse was tracked for 5 min by using a tracking program (EthoVision 9.0, Nodulus), under bright light. If a mouse fell onto the floor, the mouse was excluded from the analysis. 30 min before the test, L838,417 or vehicle was injected and experimenters were blinded to the genotypes and identity of injected drugs.

Open-field test

A mouse was placed in the middle of a square white plexiglass box (40 × 40 × 40 cm) under dim light. The movement of the mouse and location in the box was tracked using a tracking program (EthoVision 9.0, Nodulus) for 20 min. The center was defined as the middle area that occupied 1/2 of the total area. 30 min before the test, L838,417 or vehicle was injected and experimenters were blinded to the genotypes and identity of injected drugs.

Morris water maze (MWM) test

Mice were handled for 3 min on 4 consecutive days before performing the test. During training session, a mouse was placed into a white opaque water-filled (22–23 °C) tank (140 cm diameter, 100 cm height) placed in a room with multiple spatial cues under dim light. The tank was divided into 4 virtual fan-shaped quadrants, which target quadrant (TQ), opposite quadrant (OQ), adherent quadrant 1 (AQ1) and adherent quadrant 2 (AQ2). In a fixed location of TQ, a 10 cm diameter-platform was placed. On the training days, mice were pseudo-randomly released at the edge of the maze facing the inner wall of the tank and trained to reach the platform for 60 s. If the mice failed to reach the platform for 60 s, they were guided to the platform and maintained on the platform for 10 s. When the mice successfully reached the platform and stayed on the platform for more than 1 s, mice were rescued from the maze after 10 s. Mice were trained with 4 trials per day to be released at all the quadrants and the trial interval was 2 min. During the 6 consecutive training days, 30 min before the first trial, L838,417 or vehicle was injected. The day after the final day of training, a probe test was performed. In the probe test, the platform was removed and a mouse was released at the center of the pool. The mouse was tracked for 60 s with a tracking program (EthoVision 9.0, Nodulus) and, mean distance from the platform, the number of platform location crossing and time spent in each quadrant were analyzed. Experimenters were blinded to

the genotypes and identity of injected drugs.

Three-chamber test

A three-chamber apparatus was made up of successive three chambers with a door between the faced two chambers (two outer chambers: 20 x 15 x 25 cm and an inner chamber: 20 x 10 x 25 cm). Stranger mice were habituated in a metal-wired cage placed in the outer chamber for 10 min on 4 consecutive days. *Shank2* KO mice and their littermate WT mice (test mice) were also habituated in the apparatus with the doors open on two consecutive days and they had not met with the stranger mice. 24 hours after the habituation, the test mouse was placed in the inner chamber with the doors open. After 10 min, the test mouse was guided to the inner chamber and the doors were closed. A wired cup with the stranger mouse (stranger) and a wired cup with yellow block (object) were introduced into each of the outer chamber, and then the doors were opened to test sociability. The movement of the test mouse was tracked for 10 min with a tracking program (EthoVision 9.0, Nodulus). 30 min before the test, L838,417 or vehicle was injected and experimenters were blinded to the genotypes and identity of injected drugs. Experimenters were blinded to the genotypes and identity of injected drugs.

Electrophysiology

After anesthetization with isoflurane, mice were decapitated and their brains were extracted. For spontaneous/miniature and evoked IPSC experiments, 300 μm thick hippocampal slices were sectioned using a vibrating blade microtome (Leica VT1200S) and incubated in a chamber at 28 °C for at least 1 h for recovery. After the recovery period, the slices were placed in a recording chamber at 25 °C and perfused (1–1.5 ml/min) with oxygenated artificial cerebrospinal fluid (ACSF: 124 mM NaCl, 2.5 mM KCl, 1 mM NaH2PO4, 25 mM NaHCO3, 10 mM glucose, 2 mM CaCl2, and 2 mM MgSO4, 290 mOsm). For the spontaneous/miniature recording, pyramidal cells of CA1 area were recorded by whole-cell patch clamp using a glass electrode (3–4 MΩ) filled with internal solutions. One of internal solution was chosen depending on experimental conditions between Cs-gluconate internal solution containing 100 mM Cs-gluconate, 5 mM NaCl, 10 mM HEPES, 10 mM EGTA, 20 mM TEA-Cl, 3 mM QX-314, 4 mM MgATP, and 0.3 mM Na3GTP

(280–300 mOsm, pH adjusted to 7.2 with CsOH) and High-Cl internal solution containing 145 mM KCl, 5 mM NaCl, 10 mM HEPES, 10 mM EGTA, 10 mM QX-314, 4 mM MgATP, and 0.3 mM Na3GTP (280–300 mOsm pH adjusted to 7.2 with KOH). For the evoked IPSC recording, the Schaffer collateral (SC) pathway was stimulated every 20 s using concentric bipolar electrodes (MCE-100; Kopf Instruments). For E/I ratio recording, evoked excitatory currents through AMPA-R and inhibitory currents through GABA-R were recorded in the same CA1 pyramidal cells. AMPA-R-mediated currents were recorded by holding at −40 mV in AP5-containing ACSF and then switched to ACSF with AP5 and CNQX to measure GABA-R-mediated currents at holding potential of 0 mV from the same cells. About 200 μm away from the recorded cells, electronic stimulations were given to obtain approximately 300 pA of AMPA current. Experimenters were blinded to the genotypes and treatment conditions and treatment of L838,417 or vehicle was randomized by other experimenters who did not perform electrophysiological experiments.

Western Blot

After anesthetization with isoflurane, hippocampi of *Shank2* KO e6-7 or *Shank2* KO e7 with their respective littermate WT mice was extracted. Then the hippocampus in the lysis solution (30 mM Tris-Cl pH 7.4, 4 mM EDTA, 1 mM EGTA, Protease inhibitor cocktail) was homogenized with metal beads using a vibrating homogenizer (Qiagen). The homogenates were centrifuged at 500 g for 5 min at 4 °C to remove nucleus fraction. The supernatant was centrifuged at 100,000 g for 1 h at 4 °C and then the pellet was lysed in 0.5% Triton X-100 added lysis solution. The lysates were carefully loaded onto the surface of 1 M sucrose and then centrifuged again at 100,000 g for 1 h at 4 °C. Then, total protein amounts were quantified in the supernatants by the Bradford assay. Equal amounts of proteins were electrophoresed on SDS polyacrylamide gels and separated proteins were transferred onto a nitrocellulose membrane. After blocking with 5% skim milk in Tris-buffered saline plus Triton X-100 (TBST) for 2 h at room temperature, membranes were incubated with rabbit anti-GABAA-R α2 antibody (1: 2,000, R&D Systems) overnight at 4 °C. After washing with TBST buffer, the membranes were treated with an HRP-conjugated secondary antibody for 2 h at room temperature. The protein bands by HRP with enhanced

chemiluminescence reagents were detected and analyzed using the ChemiDoc (Bio-Rad) program.

Statistics

For the Morris water maze, the one-way ANOVA (analysis of variance) was performed to examine whether the mice spent significantly more time in the target quadrant than in the other three quadrants. Effects of L838,417 on different genotypes were analyzed using two-way ANOVA followed by Bonferroni post-hoc test. When two groups were compared, the unpaired two-tailed t-test was used. All data are represented as mean ± SEM and the statistical analyses were performed with Graphpad 5.0 software.

RESULTS

Comparison of transcriptomes of the two *Shank2* KO lines

It had been interesting to me that *Shank2* KO e67 mice and *Shank2* KO e7 mice have opposite physiological characteristics related with NMDA-R functions. Thus I decided to compare the two KO lines further using RNA sequencing technique. Since the previous differences in NMDA-R functions of the two KO lines were examined in the hippocampus, I made cDNA libraries from the hippocampus of the two KO mice and their respective WT littermates.

At first, RNA sequencing confirmed that exon 6 and 7 or exon 7 of *Shank2* gene was completely deleted in the two KO lines respectively (Figure 3). Next, the mRNA expression profile of each KO line was generated compared to their WT littermates in a hierarchical clustering analysis and 93 and 59 genes are identified as DEGs respectively in *Shank2* KO e67 and *Shank2* KO e7 (Figure 5, Tables 1 and 2). Furthermore, a GO enrichment analysis indicated that these DEGs were involved in lots of biological processes, including synaptic functions (Tables 3 and 4). These data showed that the two *Shank2* KO lines were differently affected by the genomic modifications in *Shank2* gene, and suggested the possibility of further differences in synaptic functions other than NMDA-R related functions.
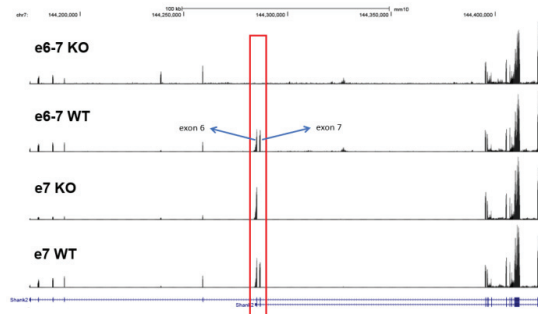
Figure 3. Confirmation of *Shank2* expression in *Shank2* KO e67 and e7 mice in RNA sequencing

(in collaboration with Dr. Jae-Hyung Lee)
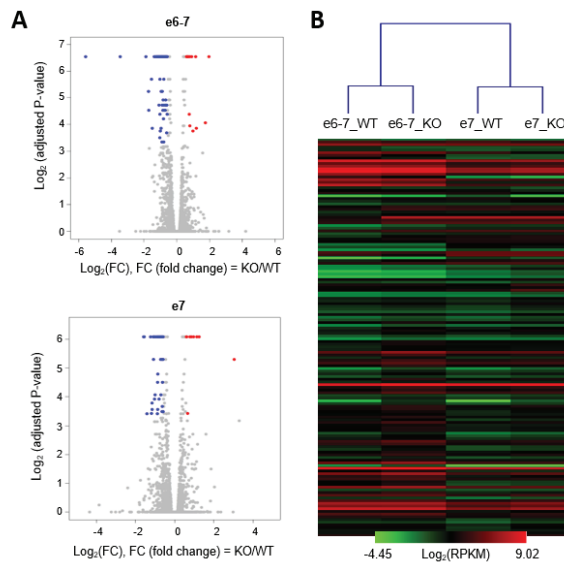
Figure 4. Differential gene expression profiles of Shank2 e67 or e7 KO lines (WT vs KO)

(A) Volcano plots showing up-regulated (Kroon et al.) and down-regulated (blue) DEGs, as the x-axis and the y-axis representing the magnitude of fold changes (log2 transformed) and adjusted p-value (-log2) respectively.

(B) A heatmap of expression levels of DEGs in four different groups (log2RPKM; reads per kilobase of exon per million mapped reads).

(in collaboration with Dr. Jae-Hyung Lee)

Table 1. Differentially expressed genes in *Shank2* KO e67 mice

Up-regulated				Down-regulated			
Ensembl ID	Gene symbol	Fold change (KO/WT)	q-value	Ensembl ID	Gene symbol	Fold change (WT/KO)	q-value
ENSMUSG00000001827	Folr1	1.760582704	0.0539673	ENSMUSG00000000560	Gabra2	1.556114264	0.0107543
ENSMUSG00000004655	Aqp1	1.726247111	0.0107543	ENSMUSG00000023484	Prph	1.691668635	0.0480958
ENSMUSG00000004885	Crabp2	2.011441807	0.074205	ENSMUSG00000026249	Serpine2	1.59349777	0.0107543
ENSMUSG00000008999	Bmp7	1.529037723	0.0378597	ENSMUSG00000031762	Mt2	1.512322684	0.0107543
ENSMUSG00000010080	Epn3	1.728306393	0.0378597	ENSMUSG00000035202	Lars2	1.567066062	0.0107543
ENSMUSG00000015090	Ptgds	1.759862849	0.0107543	ENSMUSG00000037166	Ppp1r14a	1.505765385	0.0107543
ENSMUSG00000015652	Steap1	1.94110344	0.0107543	ENSMUSG00000037541	Shank2	2.218585265	0.0107543
ENSMUSG00000015653	Steap2	1.826981468	0.0107543	ENSMUSG00000037846	Rtkn2	1.973577263	0.074205
ENSMUSG00000016024	Lbp	2.126145015	0.0107543	ENSMUSG00000059751	Rps3a3	1.876123761	0.0107543
ENSMUSG00000016918	Sulf1	2.142804157	0.0107543	ENSMUSG00000060284	Sp7	1.73045449	0.0645261
ENSMUSG00000017723	Wfdc2	1.852780533	0.0265018	ENSMUSG00000062611	Rps3a2	1.587124167	0.0107543
ENSMUSG00000019851	Perp	1.663234974	0.0107543	ENSMUSG00000065037	Rn7sk	1.721737258	0.0107543
ENSMUSG00000020473	Aebp1	1.575502452	0.0107543	ENSMUSG00000070348	Ccnd1	1.678747208	0.0107543
ENSMUSG00000020681	Ace	1.961216766	0.0107543	ENSMUSG00000092837	Rpph1	3.887519737	0.0107543
ENSMUSG00000021091	Serpina3n	2.508439252	0.0107543	ENSMUSG00000096349	Gm22513	3.335839785	0.059629
ENSMUSG00000021250	Fos	1.736252775	0.019274	ENSMUSG00000097180	2700038G22Rik	2.288290159	0.0691742
ENSMUSG00000021390	Ogn	2.0549738	0.0883393				
ENSMUSG00000021760	Gpx8	1.50652227	0.0107543				
ENSMUSG00000021848	Otx2	2.285516129	0.0107543				
ENSMUSG00000021981	Cab39l	1.603566296	0.0107543				
ENSMUSG00000022032	Scara5	2.039718414	0.0480958				
ENSMUSG00000022425	Enpp2	2.086637513	0.0107543				
ENSMUSG00000022512	Cldn1	1.716988052	0.0107543				
ENSMUSG00000022949	Clic6	2.376848584	0.0107543				
ENSMUSG00000023043	Krt18	1.607158259	0.03298				
ENSMUSG00000024610	Cd74	1.635943587	0.0432262				
ENSMUSG00000024650	Slc22a6	2.066515235	0.0107543				
ENSMUSG00000026051	1500015O10Rik	1.846678858	0.0107543				
ENSMUSG00000026579	F5	2.823764943	0.0691742				
ENSMUSG00000026822	Lcn2	3.706146729	0.0107543				
ENSMUSG00000028081	Rps3a1	47.31907609	0.0107543				
ENSMUSG00000029207	Apbb2	1.852088451	0.0378597				
ENSMUSG00000029304	Spp1	1.534366365	0.0777956				
ENSMUSG00000029661	Col1a2	1.54870461	0.0107543				
ENSMUSG00000029718	Pcolce	1.787572803	0.0107543				
ENSMUSG00000029759	Pon3	2.922372332	0.019274				
ENSMUSG00000029843	Slc13a4	2.152733902	0.0107543				
ENSMUSG00000030111	A2m	1.607718697	0.0378597				
ENSMUSG00000031070	Mrgprf	3.319762424	0.0265018				
ENSMUSG00000031095	Cul4b	1.523477296	0.0107543				
ENSMUSG00000031351	Zfp185	1.875952112	0.0985535				
ENSMUSG00000031548	Sfrp1	1.748400869	0.0107543				
ENSMUSG00000031786	Ccdc135	1.905293164	0.0107543				
ENSMUSG00000032232	Cgnl1	1.770381156	0.0107543				
ENSMUSG00000032373	Car12	1.661815248	0.0107543				
ENSMUSG00000032679	Cd59a	1.596887855	0.0378597				
ENSMUSG00000034218	Atm	3.279418451	0.0432262				
ENSMUSG00000034467	Dynlrb2	1.805464433	0.0432262				
ENSMUSG00000035493	Tgfbi	1.589166184	0.0107543				
ENSMUSG00000036103	Colec12	1.506838709	0.0480958				
ENSMUSG00000036169	Sostdc1	2.273807309	0.0107543				
ENSMUSG00000036598	Ccdc113	1.78196994	0.03298				
ENSMUSG00000037086	1110059M19Rik	2.088402803	0.0107543				
ENSMUSG00000037664	Cdkn1c	1.577660738	0.0107543				
ENSMUSG00000037738	Nek5	1.946526519	0.0691742				
ENSMUSG00000039004	Bmp6	1.970974348	0.0107543				
ENSMUSG00000039323	Igfbp2	1.635499139	0.0107543				
ENSMUSG00000039629	Strip2	1.640281015	0.0107543				
ENSMUSG00000039672	Kcne2	2.338267524	0.0107543				
ENSMUSG00000041390	Mdfic	1.865953456	0.0107543				
ENSMUSG00000041481	Serpina3g	2.12102261	0.0378597				
ENSMUSG00000041559	Fmod	1.609200398	0.0107543				
ENSMUSG00000043091	Tuba1c	1.710198754	0.0432262				
ENSMUSG00000046192	Iqub	1.742990855	0.0985535				
ENSMUSG00000046794	Ppp1r3b	2.427094026	0.0107543				
ENSMUSG00000046844	Vat1l	1.856776283	0.0107543				
ENSMUSG00000047230	Cldn2	2.262848503	0.0107543				
ENSMUSG00000048416	Mlf1	1.914330599	0.0107543				
ENSMUSG00000048450	Msx1	1.599705129	0.0107543				
ENSMUSG00000049382	Krt8	2.043581811	0.019274				
ENSMUSG00000055235	Wdr86	1.975593326	0.0107543				
ENSMUSG00000056174	Col8a2	2.004927405	0.0107543				
ENSMUSG00000058488	Kl	2.272247522	0.0107543				
ENSMUSG00000065553	Gm6969	2.598375618	0.0107543				
ENSMUSG00000068196	Col8a1	2.170067623	0.0107543				
ENSMUSG00000074825	Itpripl1	1.937585535	0.0265018				
ENSMUSG00000096999	Gm26793	10.95327203	0.0107543				

(in collaboration with Dr. Jae-Hyung Lee)

Table 2. Differentially expressed genes in *Shank2* KO e7 mice

Up-regulated				Down-regulated			
Ensembl ID	Gene symbol	Fold change (KO/WT)	q-value	Ensembl ID	Gene symbol	Fold change (WT/KO)	q-value
ENSMUSG00000004415	Col26a1	2.111546473	0.0253931	ENSMUSG00000031654	Cbln1	1.53937743	0.014728
ENSMUSG00000016024	Lbp	1.68205514	0.014728	ENSMUSG000000040380	Cbln3	8.277814964	0.0253931
ENSMUSG00000019232	Etnppl	1.642723877	0.0253931	ENSMUSG00000050919	Zfp366	1.811073378	0.014728
ENSMUSG00000020186	Csrp2	1.535861369	0.0439642	ENSMUSG00000052407	Ccdc171	2.203642206	0.014728
ENSMUSG00000020799	Tekt1	1.552070402	0.0789	ENSMUSG00000053475	Tnfaip6	1.5906793	0.0930189
ENSMUSG00000021702	Thbs4	2.943923128	0.014728	ENSMUSG00000055523	Gucy2g	1.957845606	0.014728
ENSMUSG00000021763	BC067074	1.813269043	0.0362164	ENSMUSG00000062151	Unc13c	1.516490016	0.014728
ENSMUSG00000021879	Dnah12	1.99936795	0.0597081	ENSMUSG00000065037	Rn7sk	2.381185476	0.014728
ENSMUSG00000022759	4930451C15Rik	2.119273816	0.014728	ENSMUSG00000070348	Ccnd1	1.72055618	0.014728
ENSMUSG00000022805	Maats1	1.73701956	0.014728				
ENSMUSG00000024076	Vit	1.510588805	0.0890154				
ENSMUSG00000025036	Sfxn2	1.506334319	0.0890154				
ENSMUSG00000026668	Ucma	2.350357151	0.014728				
ENSMUSG00000028294	1700003M02Rik	1.844981052	0.0938549				
ENSMUSG00000028393	Alad	1.590520537	0.014728				
ENSMUSG00000029155	Spata18	2.134177248	0.014728				
ENSMUSG00000029561	Oasl2	1.82719043	0.0439642				
ENSMUSG00000029675	Eln	1.664305178	0.014728				
ENSMUSG00000032334	Loxl1	1.62265017	0.014728				
ENSMUSG00000032680	6820408C15Rik	2.225007193	0.0727309				
ENSMUSG00000033207	Mamdc2	2.053891541	0.014728				
ENSMUSG00000033585	Ndn	1.614060885	0.014728				
ENSMUSG00000034108	Ccs	1.568453763	0.0253931				
ENSMUSG00000034227	Foxj1	1.598520228	0.014728				
ENSMUSG00000035539	E230008N13Rik	2.269367096	0.0930189				
ENSMUSG00000037016	Frem2	1.541755508	0.014728				
ENSMUSG00000037166	Ppp1r14a	1.624705237	0.0597081				
ENSMUSG00000038422	Hdhd3	1.847139723	0.014728				
ENSMUSG00000039278	Pcsk1n	1.523964187	0.014728				
ENSMUSG00000041323	Ak7	1.858334229	0.014728				
ENSMUSG00000041423	Paqr6	1.561022141	0.0890154				
ENSMUSG00000044177	Wfikkn2	1.935028748	0.014728				
ENSMUSG00000045275	Lca5l	1.732865883	0.0660872				
ENSMUSG00000046229	Scand1	2.672296336	0.0938549				
ENSMUSG00000047021	Ccdc108	1.516482658	0.014728				
ENSMUSG00000047361	Gm973	1.570890914	0.014728				
ENSMUSG00000051048	P4ha3	1.986405278	0.014728				
ENSMUSG00000052221	Ppp1r36	2.042817042	0.0660872				
ENSMUSG00000053153	Spag16	2.077070234	0.014728				
ENSMUSG00000057969	Sema3b	1.542873735	0.0253931				
ENSMUSG00000059854	Hydin	1.724471158	0.014728				
ENSMUSG00000060224	Pyroxd2	1.825014593	0.0846437				
ENSMUSG00000069917	Hba-a2	1.628708027	0.014728				
ENSMUSG00000069919	Hba-a1	1.513318861	0.014728				
ENSMUSG00000070357	E030019B06Rik	2.216894323	0.0846437				
ENSMUSG00000071398	2410004P03Rik	1.739757226	0.014728				
ENSMUSG00000072594	Gm16439	3.005447877	0.014728				
ENSMUSG00000073418	C4b	1.784132794	0.014728				
ENSMUSG00000073940	Hbb-bt	1.828051862	0.014728				
ENSMUSG00000095098	Ccdc85b	1.50937261	0.0253931				

(in collaboration with Dr. Jae-Hyung Lee)

Table 3. Gene ontology (GO) analysis on DEGs of Shank2 KO e67 mice

Up-regulated

GO ID	P-value	category	GO term	transcript ID/novel transcript	gene sysmbol
GO:0060687	<0.0001	BP	regulation of branching involved in prostate gland morpho genesis	ENSMUSG00000031548,ENSMUSG00000000899,	Sfrp1,Bmp7,
GO:0005615	<0.0001	CC	extracellular space	ENSMUSG00000015090,ENSMUSG00000041481,ENSMUSG00000022425,ENSMUSG00000039004,ENSMUSG00000026051,ENSMUSG00000031548,ENSMUSG00000021390,ENSMUSG00000021091,ENSMUSG00000016024,ENSMUSG00000035493,ENSMUSG00000029304,ENSMUSG00000026822,ENSMUSG00000002 9718,ENSMUSG00000016918,ENSMUSG00000041559,ENSMUSG00000039323,ENSMUSG00000036169,E NSMUSG00000029661,ENSMUSG00000020473,ENSMUSG00000026579,ENSMU SG00000029759,ENSMUSG00000030111,	Ptgds,Serpina3g,Enpp2,Bmp6,1S001I1SO10Rik,Sfrp1,Ogn,Serpina 3n,Lbp,Tgfbi,Spp1,Lcn2,Prolce,Sulf1,Fmod,Igfbp2,Ssstdc1,Col1a2 ,Aebp1,Bmp7,F5,Pon3,A2m,
GO:0097284	<0.0001	BP	hepatocyte apoptotic process	ENSMUSG00000023043,ENSMUSG00000049382,	Krt18,Krt8,
GO:0003094	<0.0001	BP	glomerular filtration	ENSMUSG00000034655,ENSMUSG00000016918,	Aqp1,Sulf1,
GO:0031012	<0.0001	CC	extracellular matrix	ENSMUSG00000068196,ENSMUSG00000031548,ENSMUSG00000021390,ENSMUSG00000035493,ENSM USG00000029718,ENSMUSG00000056174,ENSMUSG00000041559,ENSMUSG00000029661,ENSMUSG00 000020473,ENSMUSG00000000899,	Col8a1,Sfrp1,Ogn,Tgfbi,Prolce,Col8a2,Fmod,Col1a2,Aebp1,Bmp7,
GO:0048593	<0.0001	BP	camera-type eye morphogenesis	ENSMUSG00000068196,ENSMUSG00000056174,ENSMUSG00000004655,ENSMUSG00000000899,	Col8a1,Col8a2,Aqp1,Bmp7,
GO:0070062	<0.0001	CC	extracellular vesicular exosome	ENSMUSG00000035493,ENSMUSG00000029718,ENSMUSG00000004655,ENSMUSG00000029661,ENSM USG00000030111,	Tgfbi,Prolce,Aqp1,Col1a2,A2m,
GO:0060395	0.0001	BP	SMAD protein signal transduction	ENSMUSG00000039004,ENSMUSG00000000899,ENSMUSG00000021250,	Bmp6,Bmp7,Fos,
GO:0060686	0.0001	BP	negative regulation of prostatic bud formation	ENSMUSG00000016918,ENSMUSG00000000899,	Sulf1,Bmp7,
GO:0005215	0.0001	MF	transporter activity	ENSMUSG00000015653,ENSMUSG00000015090,ENSMUSG00000004885,ENSMUSG00000026822,ENSM USG00000004655,ENSMUSG00000029843,	Steap2,Ptgds,Crabp2,Lcn2,Aqp1,Slc13a4,
GO:0030501	0.0001	BP	positive regulation of bone mineralization	ENSMUSG00000058488,ENSMUSG00000039004,ENSMUSG00000000899,	Kl,Bmp6,Bmp7,
GO:0031988	0.0001	CC	membrane-bounded vesicle	ENSMUSG00000039004,ENSMUSG00000029304,ENSMUSG00000000899,	Bmp6,Spp1,Bmp7,
GO:0043066	0.0002	BP	negative regulation of apoptotic process	ENSMUSG00000031548,ENSMUSG00000048450,ENSMUSG00000023043,ENSMUSG00000029304,ENSMUSG00000056174,ENSM USG00000024610,ENSMUSG00000004655,ENSMUSG00000029207,	Sfrp1,Msx1,Krt18,Spp1,Cd74,Aqp1,Apbb2,
GO:0007155	0.0002	BP	cell adhesion	ENSMUSG00000016918,ENSMUSG00000035493,ENSMUSG00000056174,ENSMUSG00000020473,ENSMUSG00000026579,	Col8a1,Tgfbi,Spp1,Col8a2,Sulf1,Aebp1,F5,
GO:0005581	0.0002	CC	collagen	ENSMUSG00000068196,ENSMUSG00000036103,ENSMUSG00000056174,ENSMUSG00000029661,	Col8a1,Colec12,Col8a2,Col1a2,
GO:0051216	0.0002	BP	cartilage development	ENSMUSG00000039004,ENSMUSG00000048450,ENSMUSG00000016918,ENSMUSG00000000899,	Bmp6,Msx1,Sulf1,Bmp7,
GO:0007050	0.0003	BP	cell cycle arrest	ENSMUSG00000024218,ENSMUSG00000048416,ENSMUSG00000029207,ENSMUSG00000037664,	Atm,Mlf1,Apbb2,Cdkn1c,
GO:0070700	0.0003	MF	BMP receptor binding	ENSMUSG00000039004,ENSMUSG00000000899,	Bmp6,Bmp7,
GO:0050673	0.0005	BP	epithelial cell proliferation	ENSMUSG00000068196,ENSMUSG00000056174,	Col8a1,Col8a2,
GO:0005576	0.0006	CC	extracellular region	ENSMUSG00000015090,ENSMUSG00000041481,ENSMUSG00000058488,ENSMUSG00000017723,ENSM USG00000021091,ENSMUSG00000029304,ENSMUSG00000026822,ENSMUSG00000029718,ENSMUSG000 00035923,ENSMUSG00000030111,ENSMUSG00000026581,	Ptgds,Serpina3g,Kl,Wfdc2,Serpina3n,Spp1,Lcn2,Prolce,Igfbp2,A2 m,Ace,
GO:0071347	0.0006	BP	cellular response to interleukin-1	ENSMUSG00000031548,ENSMUSG00000021091,ENSMUSG00000026822,	Sfrp1,Serpina3n,Lcn2,
GO:0036094	0.0006	MF	small molecule binding	ENSMUSG00000015090,ENSMUSG00000026822,	Ptgds,Lcn2,
GO:0001822	0.0007	BP	kidney development	ENSMUSG00000039004,ENSMUSG00000016918,ENSMUSG00000000899,ENSMUSG00000002681,	Bmp6,Sulf1,Bmp7,Ace,
GO:0004867	0.0008	MF	serine-type endopeptidase inhibitor activity	ENSMUSG00000041481,ENSMUSG00000017723,ENSMUSG00000021091,ENSMUSG00000030111,	Serpina3g,Wfdc2,Serpina3n,A2m,
GO:0090023	0.0009	BP	positive regulation of neutrophil chemotaxis	ENSMUSG00000016024,ENSMUSG00000024610,	Lbp,Cd74,

Down-regulated

GO ID	P-value	category	GO term	transcript ID/novel transcript	gene sysmbol
GO:0005883	<0.0001	CC	neurofilament	ENSMUSG00000023484,ENSMUSG00000037541,	Prph,Shank2,
GO:0022627	0.0015	CC	cytosolic small ribosomal subunit	ENSMUSG00000062611,ENSMUSG00000059751,	Rps3a2,Rps3a3,
GO:0030154	0.0019	BP	cell differentiation	ENSMUSG00000026249,ENSMUSG00000062611,ENSMUSG00000059751,	Serpine2,Rps3a2,Rps3a3,
GO:0045211	0.0026	CC	postsynaptic membrane	ENSMUSG00000000560,ENSMUSG00000037541,	Gabra2,Shank2,
GO:0030424	0.0048	CC	axon	ENSMUSG00000023484,ENSMUSG00000000560,	Prph,Gabra2,

(in collaboration with Dr. Jae-Hyung Lee)

Table 4. GO analysis on DEGs of Shank2 KO e7 mice

Up-regulated

GO ID	P-value	category	GO term	transcript ID/novel transcript	gene sysmbol
GO:0019825	<0.0001	MF	oxygen binding	ENSMUSG00000073940,ENSMUSG00000069919,ENSMUSG00000069917,	Hbb-bt,Hba-a1,Hba-a2,
GO:0005833	<0.0001	CC	hemoglobin complex	ENSMUSG00000073940,ENSMUSG00000069919,ENSMUSG00000069917,	Hbb-bt,Hba-a1,Hba-a2,
GO:0005344	<0.0001	MF	oxygen transporter activity	ENSMUSG00000073940,ENSMUSG00000069919,ENSMUSG00000069917,	Hbb-bt,Hba-a1,Hba-a2,
GO:0042384	0.0003	BP	cilium assembly	ENSMUSG00000005153,ENSMUSG00000059854,ENSMUSG00000034227,	Spag16,Hydin,Foxj1,
GO:0005539	0.0004	MF	glycosaminoglycan binding	ENSMUSG00000033207,ENSMUSG00000024076,	Mamdc2,Vit,
GO:0005614	0.0005	CC	interstitial matrix	ENSMUSG00000033207,ENSMUSG00000016024,	Mamdc2,Vit,
GO:0090023	0.0005	BP	positive regulation of neutrophil chemotaxis	ENSMUSG00000021702,ENSMUSG00000016024,	Thbs4,Lbp,
GO:0005506	0.0006	MF	iron ion binding	ENSMUSG00000073940,ENSMUSG00000051048,ENSMUSG00000069919,ENSMUSG00000069917,	Hbb-bt,Hba3,Hba-a1,Hba-a2,
GO:0005578	0.001	CC	proteinaceous extracellular matrix	ENSMUSG00000032334,ENSMUSG00000026668,ENSMUSG00000004415,ENSMUSG00000029675,	Loxl1,Ucma,Col26a1,Efn,
GO:0031012	0.0012	CC	extracellular matrix	ENSMUSG00000033207,ENSMUSG00000032334,ENSMUSG00000026668,ENSMUSG00000024076,	Mamdc2,Loxl1,Ucma,Vit,
GO:0010811	0.0022	BP	positive regulation of cell-substrate adhesion	ENSMUSG00000004415,ENSMUSG00000024076,	Col26a1,Vit,
GO:0004864	0.0029	MF	protein phosphatase inhibitor activity	ENSMUSG00000052221,ENSMUSG00000037166,	Ppp1r36,Ppp1r14a,

Down-regulated

GO ID	P-value	category	GO term	transcript ID/novel transcript	gene sysmbol
GO:0043627	0.0003	BP	response to estrogen stimulus	ENSMUSG00000070348,ENSMUSG00000050919,	Ccnd1,Zfp366,
GO:0030054	0.0003	CC	cell junction	ENSMUSG00000062151,ENSMUSG00000040380,ENSMUSG00000031654,	Unc13c,Cbln3,Cbln1,
GO:0045202	0.0044	CC	synapse	ENSMUSG00000040380,ENSMUSG00000031654,	Cbln3,Cbln1,
GO:0035556	0.0071	BP	intracellular signal transduction	ENSMUSG00000062151,ENSMUSG00000055523,	Unc13c,Gucy2g,

(in collaboration with Dr. Jae-Hyung Lee)

Among the DEGs, mRNA expression of *Gabra2* was significantly down-regulated in *Shank2* KO e67 mice, but not in *Shank2* KO e7 mice. Based on this result, I performed quantitative RT-PCR to evaluate the mRNA expression of genes related to postsynaptic functions (Figure 5A, B). I confirmed that the mRNA expression of *Gabra2* was significantly reduced only in *Shank2* KO e67 mice. In addition, mRNA expression of a gene encoding the subunit 1 of NMDA-R (Grin1) was reduced in *Shank2* KO e67 mice, but not in *Shank2* KO e7 mice. mRNA expression of a gene encoding the subunit 1 of AMPA-R (Gria1) and a gene encoding a postsynaptic density protein, Dlg4, were increased in *Shank2* KO e7 mice, but not in *Shank2* KO e67 mice. However, the alterations in the mRNA expression of *Grin1*, *Gria1* and *Dlg4* were not that dramatic and I focused *Gabra2*. To evaluate the GABAAα2 protein level, I performed western blot analysis in the hippocampus of the *Shank2* KO e67 mice. Since GABAAα2 is primarily located in postsynaptic area, I extracted the synaptic fraction from the hippocampus and found that GABAAα2 was significantly decreased in *Shank2* KO e67 mice compared to their WT littermates (Figure 5C, D).

In addition, we found another difference between the two *Shank2* KO lines. An unknown transcript of *Shank2* is expressed only in *Shank2* KO e67 mice, which starts from center of exon 8 and expanded to exon 16 without SH3 and PDZ domains (data not shown). However, since it was not certain whether the transcript is really expressed as a protein, I focused on the difference level of *Gabra2* expression.
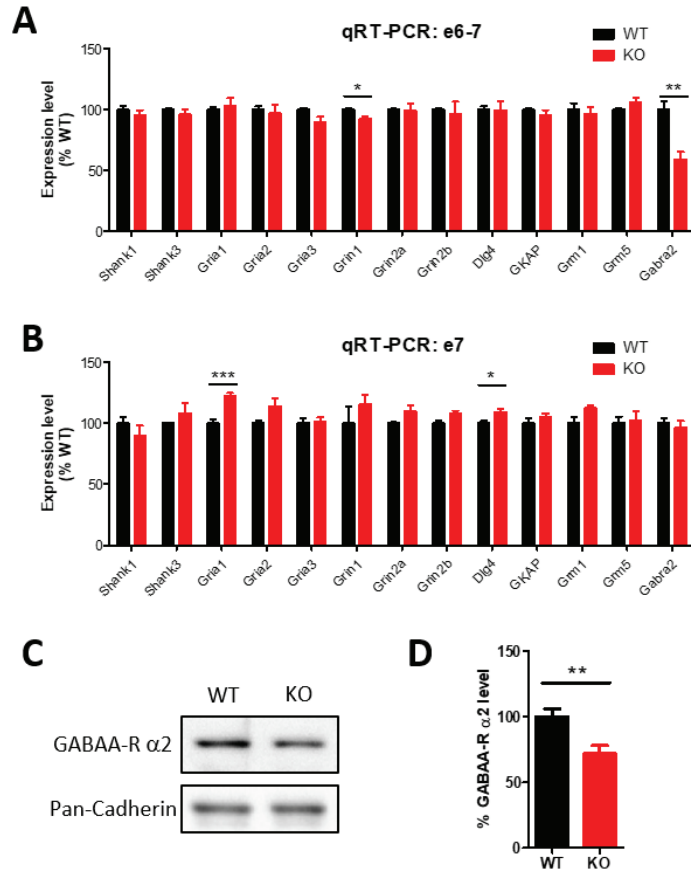
Figure 5. Decreased *Gabra2* expression in mRNA and protein level

(A, B) qRT-PCR analyses to evaluate the expression level of postsynaptic genes from the hippocampus of *Shank2* KO e67 and e7 mice (WT: n = 3, KO: n = 3, unpaired t-test *P < 0.05, **P < 0.01). (C, D) Reduced expression of GABAAα2 in the hippocampus of *Shank2* KO e67 mice. Pan-cadherin was used as internal control and the expression levels of GABAA α2 subunit are normalized by the intensity of (WT: n = 8, KO: n = 6, unpaired t-test **P < 0.01).

(in collaboration with Dr. Nam-Kyung Yu Dr. Hyoung-Gon Ko)

Functional identification of decreased GABAAα2 in *Shank2* KO e67 mice

I found that the expression of GABAAα2 was reduced only in the *Shank2* KO e67 mice. GABAA receptors are localized in both synaptic and extrasynaptic sites and primarily involved in the inhibitory neurotransmission in the cortex and hippocampus (Benarroch, 2007). Thus I expected that the inhibitory transmission of *Shank2* KO e67 mice was impaired, changing the normal E/I balanced states.

To examine it, GABAergic inhibitory currents were recorded from CA1 pyramidal neurons using whole-cell patch clamp while the Schaffer collateral pathway was stimulated with varying intensities (input-output relationship). Consistently with the decreased expression of GABAα2, the amplitude of inhibitory currents was slightly, but significantly reduced in the *Shank2* KO e67 mice compared to their WT littermates (Figure 6A) On the other hand, the input-output relationship of inhibitory currents of the *Shank2* KO e7 mice was comparable to their WT littermates (Figure 6B). The reduced inhibitory transmission in *Shank2* KO e67 mice could be resulted from general impairment of neurotransmission. Thus, the AMPA-R mediated excitatory transmission was also examined and AMPA-R currents was not affected by *Shank2* KO in both lines (Figure 6C). As a result, the E/I ratio was increased in the *Shank2* KO e67 mice, while the ratio was not altered in the *Shank2* KO e7 mice (Figure 6D).

To further confirm whether the change in inhibitory currents are resulted from an impairment in GABAA functions by reduced GABAα2, a GABAA receptor agonist, especially containing α2 subunit, L838,417, was treated during the patch clamp recording. The AMPA-R mediated currents were not affected, while the reduced GABA-R currents and E/I ratio of Shank2 KO e67 mice were restored being comparable to those of WT littermates. The GABA-R currents of WT mice were not increased by L838,417 and it might be resulted from the ceiling effect (Figure 6C, D).

36
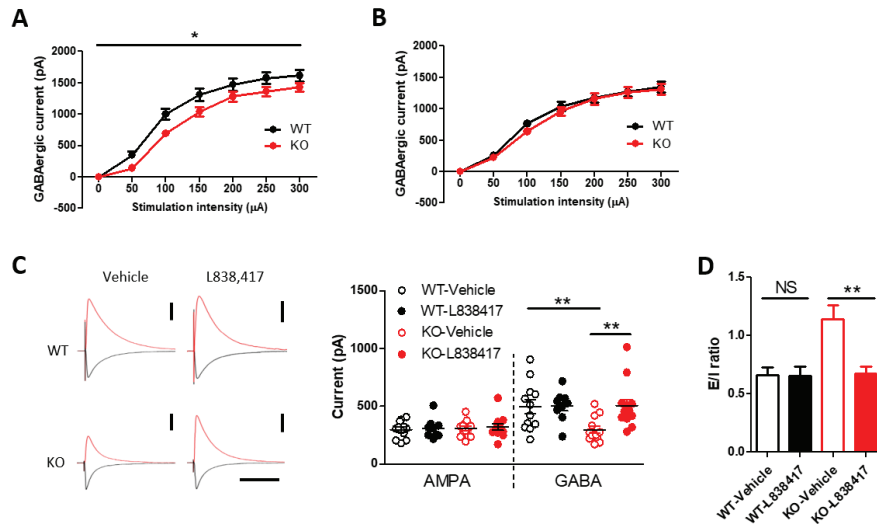
Figure 6. Decreased inhibitory GABAergic function and rescue of it by L838,417 in *Shank2* e67 KO mice

(A) Decreased GABAergic current in input-output relationships of CA1 neurons of *Shank2* KO e67 mice compared to WT littermates (WT-Vehicle: n = 27 cells/6 animals; KO-Vehicle: n = 28 cells/6 animals; two-way ANOVA, genotype x intensity interaction, $^*P < 0.05$). (B) Normal GABAergic current in input-output relationships of CA1 neurons of *Shank2* KO e7 mice (WT: n = 21 cells/4 animals; KO: n = 20 cells/4 animals; two-way ANOVA, genotype x intensity interaction, P = 0.743). (C) Representative traces (left) and plot (right) of AMPAR or GABAR mediated currents from CA1 neurons of *Shank2* KO e67 mice after treatment with vehicle or L838,417 (GABAR currents, WT-Vehicle vs. KO-Vehicle, unpaired t-test, $^{**}P < 0.01$; KO-Vehicle vs. KO-L838,417, unpaired t-test, $^{**}P < 0.01$). Scale bar: 200 pA, 100 msec. (D) Increased E/I ratios in CA1 neurons in *Shank2* KO e67 mice compared to WT littermates. The E/I ratio was rescued by L838,417 treatment (WT-Vehicle: n = 12 cells/5 animals; KO-Vehicle: n = 13 cells/5 animals; WT-L838,417: n = 9 cells/4 animals; KO-L838417: n = 13 cells/5 animals; two-way ANOVA, effect of genotype, $^*P < 0.05$, Bonferroni posttests, KO-Vehicle vs. KO-L838,417, $^{**}P < 0.01$). NS, not significant.

(in collaboration with Dr. Chae-Seok Lim)

In addition to the evoked transmissions, spontaneous miniature EPSC (mEPSC) and IPSC (mIPSC) were also recorded in CA1 pyramidal cells since in many neurodevelopmental disorders, the frequency or amplitude of the spontaneous postsynaptic currents are also perturbed (Gkogkas et al., 2013; Han et al., 2012; Kim et al., 2016; Lee et al., 2017). The frequency or amplitude of mEPSC and mIPSC of *Shank2* KO were not significantly different from those of WT littermates (Figure 7A, B). Presynaptic release probability was also examined by paired-pulse ratio (PPR) in the CA1 pyramidal cells at two stimulation intervals (70 ms and 150 ms) and at both intervals, the PPR was not different between *Shank2* KO e67 mice and WT littermates (Figure 7C).
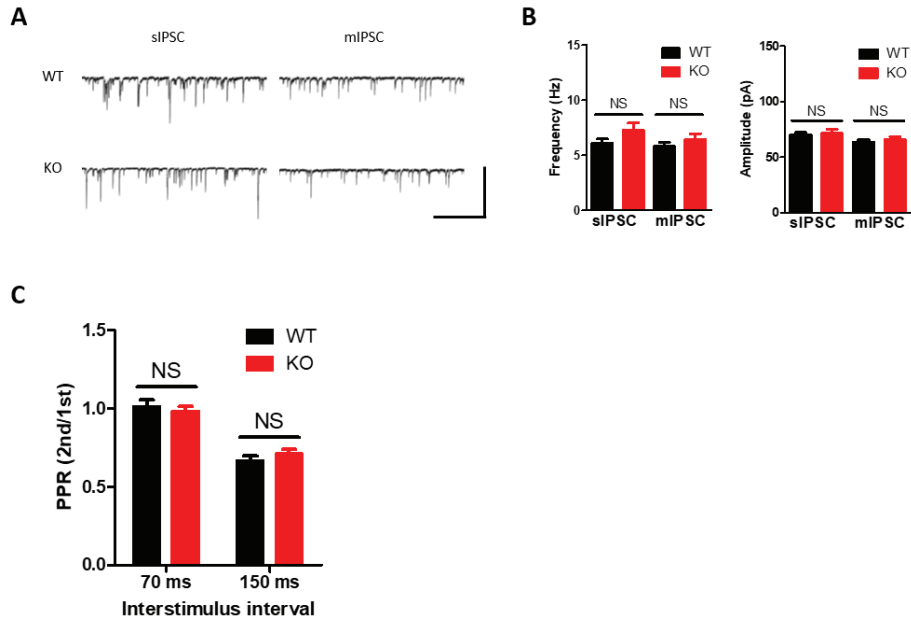
Figure 7. Recording of spontaneous mEPSC or mIPSC, and paired-pulse facilitation ratios (PPR)

(A, B) Normal spontaneous and miniature inhibitory postsynaptic currents (sIPSC and mIPSC) in *Shank2* KO e67 mice compared with WT littermates (sIPSC, WT: n = 26; KO: n = 25; mIPSC, WT: n = 21; KO: n = 18 cells). Scale bar: 300 pA, 2 s. (C) Normal paired-pulse facilitation ratios (PPR) in *Shank2* KO e67 mice compared with WT littermates (70 ms, WT: n = 13; KO: n = 14; 150 ms, WT: n = 9; KO: n = 12 cells; two-way ANOVA, genotype: $F_{1,44} = 0.03$, $P = 0.855$). NS, not significant

(in collaboration with Dr. Chae-Seok Lim)

Effects of L838,417 in the social behaviors of *Shank2* KO e67 mice.

Alterations in E/I balance are frequently observed phenomena in the animal models of neurodevelopmental disorders (Lee et al., 2017; Peñagarikano et al., 2011; Schmeisser et al., 2012; Won et al., 2012; Yizhar et al., 2011), and suggested as one of underlying physiological mechanism of the cognitive deficits of the disorders. Previously, *Shank2* KO e67 mice are characterized by autistic behaviors such as social deficits and repetitive jumping behaviors, and enhancing NMDA-R function partially improved social behaviors of *Shank2* KO e67 mice (Won et al., 2012). To estimate if restoring the E/I balance by enhancing GABAA-R function also could rescue the social deficits of the mice, I performed three-chamber test after treating L838,417 in the *Shank2* KO e67 mice. Consistently with the previous report, the sociability of *Shank2* KO e67 mice was significantly impaired compared to that of WT littermate mice, however, the impaired sociability was not rescued by the L838,417 treatment (Figure 8). The result suggests that the decreased GABAA-R function may not attribute to the social deficits in the *Shank2* KO e67 mice.
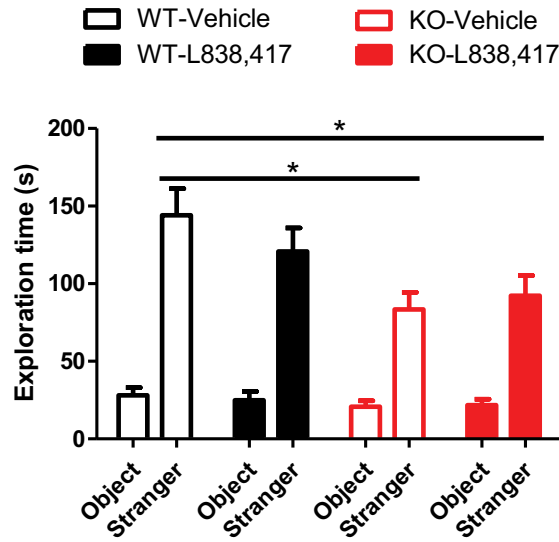
Figure 8. Effects of L838,417 treatment on impaired social behaviors of *Shank2* KO e67 mice

L838,417 did not affect the sociability of *Shank2* KO e67 mice in the three-chamber test (WT-Vehicle: n = 9; WT-L838,417: n = 8; KO-Vehicle: n = 8; KO-L838,417: n = 7; unpaired t-test, *P < 0.05).

Effects of L838,417 in spatial memory deficits of *Shank2* KO e67 mice.

Individuals of ASD are suffer from various cognitive deficits such as anxiety, learning and memory deficits, as well as the impaired social behaviors. *Shank2* KO e67 mice also displays spatial learning and memory deficits (Won et al., 2012). I focused on the spatial learning and memory, since intellectual disabilities are frequently accompanied with the ASD patients. In addition, imbalances of the E/I balance in the hippocampus have also been reported to be involved in the learning and memory deficits (Cui et al., 2008; Han et al., 2014; Han et al., 2012; Houbaert et al., 2013; Lee et al., 2014).

I examined whether the spatial learning and memory deficits of *Shank2* KO e67 mice in Morris-water maze could be restored by the L838,417 treatments. As previously reported, vehicle treated *Shank2* KO e67 mice did not acquire the position of the hidden platform well compared to WT littermate mice during the training sessions (Figure 9A). L838,417 treated *Shank2* KO e67 mice also could not find the platform well and the latency to find the platform was not significantly different from that of vehicle treated *Shank2* KO e67 mice. L838,417 treated WT littermate mice learned the position of the platform well. In the probe test, WT littermate mice spent significantly more time in the target quadrant where the platform was located during the training sessions, while vehicle treated *Shank2* KO e67 mice randomly went around the pool and spent similar time in each quadrant. On the other hand, L838,417 treated *Shank2* KO e67 mice spent significantly more time in the target quadrant (Figure 9B). Moreover, the mean distance from the center of the platform was significantly higher in the vehicle treated *Shank2* KO e67 mice group compared to the L838,417 treated group (Figure 9C). The mean swimming velocity was comparable in all groups, suggesting that these results were not coming from the alterations on locomotive properties (Figure 9D).
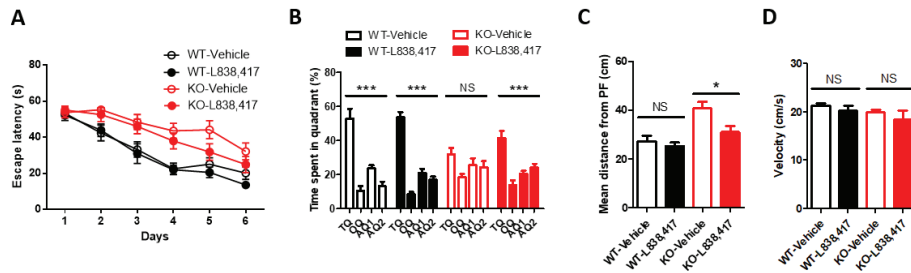
Figure 9. Effects of L838,417 treatment on spatial memory deficits of *Shank2* KO e67 mice

(A) Learning curve of *Shank2* KO e67 mice in the Morris water maze task (WT-Vehicle vs KO-Vehicle, two-way ANOVA, genotype: $F_{1,90} = 17.74$, $P < 0.001$; KO-Vehicle vs KO-L838,417, two-way ANOVA, treatment: $F_{1,100} = 1.704$, $P > 0.05$). (B) Time spent in each quadrant during probe test, 24 h after training (WT-Vehicle: n = 9; WT-L838,417: n = 8; KO-Vehicle: n = 11; KO-L838,417: n = 11; one-way ANOVA of KO-Vehicle, NS; one-way ANOVA of KO-L838,417, ***$P < 0.001$). TQ: target, OQ: opposite, AQ1: right, AQ2: left quadrant. (C) Enhanced spatial memory of *Shank2* e67 KO mice in mean distance from the platform during probe test by L838,417 (WT-Vehicle: n = 9; WT-L838,417: n = 8; KO-Vehicle: n = 11; KO-L838,417: n = 11, two-way ANOVA followed by Bonferroni posttests, *$P < 0.05$). (D) Swimming velocity of *Shank2* KO e67 mice was comparable with WT littermates during probe test (WT-Vehicle: n = 9; WT-L838,417: n = 8; KO-Vehicle: n = 11; KO-L838,417: n = 11, unpaired t-test). NS, not significant.

43

I examined spatial memory of *Shank2* KO e7 mice in the Morris-water maze task either, to address whether the mice also show deficits in spatial learning and memory. In spite of the normal E/I ratio of them, the *Shank2* KO e7 mice also showed a tendency of deficit during the training days (Figure 10A). Furthermore, vehicle treated *Shank2* KO e7 mice randomly swam around the four quadrants, while WT littermates spent significantly more time in the target quadrant during the probe test. The results indicated that the spatial memory of *Shank2* KO e7 mice is also impaired (Figure 10B).

If the rescue effect of L838,417 in *Shank2* KO e67 mice was really resulted from the restoring of E/I balance, I expected that the drug should have no memory rescue effect in *Shank2* KO e7 mice. As I expected, when I treated L838,417 in Shank KO e7 mice, contrary to e6-7 KO mice, the mice did not show a preference for the target quadrant, still randomly swimming around the four quadrants during the probe test (Figure 10B). In addition, the mean distance from platform position was comparable between the L838,417-treated *Shank2* KO e7 mice group and the vehicle treated group, suggesting that L838,417 did not rescue the impaired spatial memory of *Shank2* KO e7 mice (Figure 10C). As in the *Shank2* KO e67 mice, L838,417 treatment did not affect the swimming velocity (Figure 10D). Taken together, these results suggest that the spatial memory deficits of *Shank2* KO e7 mice was not resulted from the GABAA-R functions, but from other mechanisms, while the alteration of GABAA-R functions is attributable for the spatial memory deficits of *Shank2* KO e67 mice.
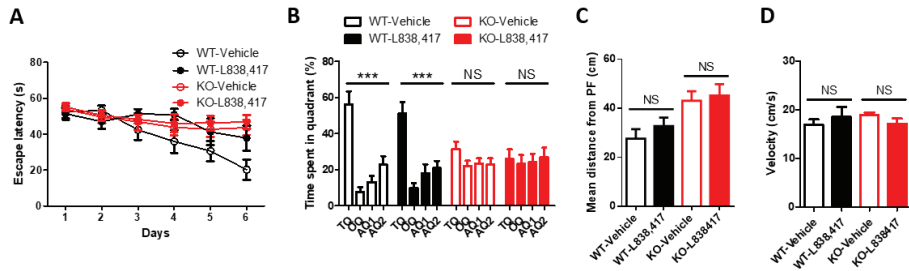
Figure 10. Effects of L838,417 treatment on spatial memory deficits of *Shank2* KO e7 mice

(A) Learning curve of *Shank2* KO e7 mouse line during training in the Morris water maze task (WT-Vehicle vs KO-Vehicle, two-way ANOVA, effect of genotype, P = 0.146; KO-Vehicle vs KO-L838,417, two-way ANOVA, effect of treatment: P = 0.639). (B) Time spent in each quadrant during probe test, 24 h after training (WT-Vehicle: n =10; WT-L838,417: n = 6; KO-Vehicle: n = 12; KO-L838,417: n = 11; one-way ANOVA of WT-Vehicle, *** P < 0.001; WT-838,417, *** P < 0.001; KO-Vehicle, P = 0.168; KO-L838,417, P = 0.961). TQ: target, OQ: opposite, AQ1: right, AQ2: left quadrant. (C) L838,417 did not improve mean distance from the platform of *Shank2* e7 during probe (WT-Vehicle: n = 10; WT-L838,417: n = 6; KO-Vehicle: n = 12; KO-L838,417: n = 11, two-way ANOVA, effect of genotype, P < 0.01; effect of treatment, P = 0.404). (D) Swimming velocity of *Shank2* KO e7 mice was comparable with WT littermates during probe test (WT-Vehicle: n = 10; WT-L838,417: n = 6; KO-Vehicle: n = 12; KO-L838,417: n = 11, unpaired t-test). *(in collaboration with Jaehyun Lee)*

45

Effects of L838,417 in emotional status and locomotion of *Shank2* KO e67 mice.

In addition to the behavioral tests involved in sociability and spatial memory, I performed elevated zero-maze task and open-field test to examine effects of L838,417 on the emotional states or locomotion (Figure 11 A, B). In the elevated zero-maze, time in open area of vehicle treated *Shank2* KO e67 mice was significantly different with that of vehicle treated WT littermates. L838,417 treated *Shank2* KO e67 mice also spent comparable time with the vehicle treated *Shank2* KO e67 group. Similarly, in the open-field test, the center duration of L838,417 treated *Shank2* KO e67 group was not different from that of vehicle treated KO group. These results suggest that L838,417 treatment did not affect the anxiety of the *Shank2* KO e67 mice. In relation with locomotion, in both elevated zero-maze and open-field test, the hyperactivity of *Shank2* KO e67 was tended to reduce by L838,417 but it was not statistically significant.

Taken together, our results suggest that restoring GABAergic synaptic transmission and E/I balance using L838,417 could ameliorate the spatial memory deficit of *Shank2* e6-7 KO mice, without affecting the social or emotional behaviors of the KO mice.
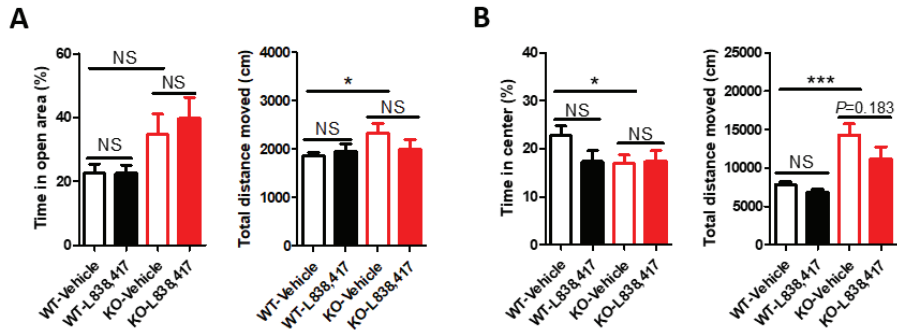
Figure 11. Effects of L838,417 on anxiety like behavior and locomotor activity of *Shank2* KO e67 mice

(A) No changes in basal anxiety level of *Shank2* e6-7 KO mice and WT littermates following administration of L838,417 in the elevated zero-maze (EZM) test (left, WT-Vehicle: n = 11; WTL838,417: n = 10, KO-Vehicle: n = 8; KO-L838,417: n = 7; two-way ANOVA, interaction, $F_{1,32} = 0.339$, $P = 0.564$) while locomotor activity was significantly increased compared with WT littermates (right, WT-Vehicle vs. KO-Vehicle, unpaired t-test, * $P < 0.05$). (B) In the open-field test, *Shank2* e6-7 KO mice showed significantly decreased time spent in the center region compared with WT littermates (left, WT-Vehicle: n = 11; WT-L838,417: n = 10; KO-Vehicle: n = 8; KO-L838,417: n = 7, KO-Vehicle vs KO-L838,417, unpaired t-test, * $P < 0.05$), while locomotor activity was significantly increased compared with WT littermates (right, WT-Vehicle vs KO-Vehicle, unpaired t-test, *** $P < 0.001$), which was partially rescued by L838,417 administration (KO-Vehicle vs. KO-L838,417, unpaired t-test, $P = 0.183$). NS, not significant.

DISCUSSION

In the present study, I showed that two *Shank2* KO mice (e67 and e7) are different at the transcriptome level, where the level of *Gabra2* mRNA was reduced in the hippocampus of *Shank2* KO e67 mice, but not in *Shank2* KO e7 mice. This result provides a new evidence that the two KO lines are different even if the deleted gene is same. Consistently with the reduction of *Gabra2* expression in *Shank2* KO e67 mice, inhibitory GABA current was also reduced making elevated E/I ratio. Treatment of L838,417, a positive allosteric modulator of α2, α3, and α5-specific GABAA-R, restored the reduced GABA current and normalized the E/I ratio in *Shank2* KO e67 mice. Finally, administration of L838,417 enhanced hippocampus dependent spatial memory deficit but not the social deficit of *Shank2* e67 KO mice. These findings uncover a novel mechanism underlying the spatial memory deficit in *Shank2* KO e67 mice.

Brain regions involved in the spatial deficits of *Shank2* KO e67 mice

Since I systemically injected L838,417, the drug could affect many areas of brain. However, since hippocampus was a primary brain region involved with spatial memory (Olton and Paras, 1979; Tsien et al., 1996), and all the molecular biological and physiological experiments are done using hippocampus, I think that the spatial memory rescue effect of L838,417 was hippocampus dependent. In relation with the social behaviors, many other brain regions are involved including medial prefrontal cortex, amygdala and nucleus accumbens hippocampus (Gunaydin et al., 2014; Schoch et al., 2017; Selimbeyoglu et al., 2017), so the E/I balance or GABAergic functions may be differently regulated in the areas compared to. Investigating the molecular profile or physiological characteristics of the other regions in *Shank2* KO mice would provide further understanding of the social deficits of the mice.

Mutations in same gene, but different phenotypes

Consistently with the reduced *Gabra2* expression only in *Shank2* KO e67 mice, L838,417

treatment rescued the spatial memory deficits only in e67 KO, but not in e7 KO mice. In addition to the different expression of *Gabra2*, *Shank2* e67 KO and e7 KO mice showed differences in the NMDAR functions previously (Schmeisser et al., 2012; Won et al., 2012). There are other examples which show that different mutations in the same gene could cause distinct phenotypes. *Shank3* e4-9 KO mice have impaired spatial memory (Wang et al., 2011), whereas *Shank3* e13-16 KO mice (Peça et al., 2011) have normal spatial memory. *Shank3* e13-16 KO mice also have distinct cellular phenotypes from Shank3 e4-9 KO mice. Moreover, mice with different mutations in *Shank3*, show distinct behavioral deficits (Zhou et al., 2016). In addition, two different mutations of *MECP2* (*MeCP2*-R270X and *MeCP2*-G273X) which is implicated in Rett Syndrome, a kind of autism spectrum disorders, differentially affected the function of MECP2 and making distinct bending patterns of the protein (Baker et al., 2013). Mice with each mutation also showed different severity of phenotypes, which is similar to the disease progression observed in the patients with the two mutations (Baker et al., 2013).

It is not easy to say how the two *Shank2* KO lines have different molecular and physiological phenotypes. When we target a gene to be mutated, we mostly focused only exons and known transcripts, but we don't know the complex regulation of genome perfectly. For example, the transcription of targeted gene by KO strategy might be complicated generating a novel transcript. These possibilities should be addressed sometime.

E/I balance in ASD

Maintaining proper E/I balance is required for normal social behaviors and cognitive functions (Lee et al., 2017; Yizhar et al., 2011). Recent studies have highlighted that imbalance of E/I ratio as a common physiological mechanism underlying behavioral deficits of animal models of ASD. Indeed, a number of ASD model mice apart from *Shank2* KO mice, are also characterized by alterations in E/I balance, sometimes increasing, other times decreasing (Chao et al., 2010; Etherton et al., 2009; Gkogkas et al., 2013; Han et al., 2014; Han et al., 2012; Hines et al., 2008; Hung et al., 2008).

Especially, GABAergic transmission is a major inhibitory mechanism of brain and many ASD model mice are characterized by alteration in GABAergic systems (Cellot and Cherubini, 2014,

Chao et al., 2010, Han et al., 2012, Han et al., 2014, Oblak et al., 2011, Robertson et al., 2016). Although Shank proteins are mainly localized in excitatory postsynaptic density, I found that GABAergic currents were decreased in *Shank2* e67 KO mice, suggesting the role of *Shank2* in GABAergic systems. Supporting the role, expression of parvalbumin, a marker for a subpopulation of GABAergic neurons, was also decreased in *Shank1* KO and *Shank3B* KO mice (Filice et al., 2016).

Molecular mechanisms related with reduced *Gabra2* in *Shank2* KO e67 mice

Because Shank2 is a scaffolding protein and do not directly regulate gene expression itself, it is unclear how the lack of *Shank2* expression in *Shank2* e67 KO mice affected *Gabra2* expression. One possible molecular target is the Janus kinase signal transducer and activator of transcription (STAT) signaling pathway. STAT protein is a well-known transcription modulator and there are some evidences that STAT might affect the expression of genes involved in excitatory and inhibitory neurotransmissions in *Shank2* KO e67 mice. For example, it was reported that JAK2 and STAT3 are required for NMDAR-dependent LTD in hippocampus, and STAT3 regulates expression of GABAA receptor subunits in hippocampus (Lund et al., 2008; Nicolas et al., 2012). Since NMDAR-dependent LTD in hippocampus was diminished in *Shank2* KO e67 mice (Won et al., 2012) and *Gabra2* expression was also decreased in the mouse line, the JAK/STAT pathway might be responsible for the impairments of *Shank2* e67 KO mice considering the function of it.

CHAPTER III

Role of *Snf7-3* in neurodevelopmental disorders regulating the

dendritic developmental processes

INTRODUCTION

Snf7-3 is a protein which is a member of Snf7 family, and also known as chromatin-modifying protein/charged multivesicular body protein 4C (CHMP4C). Snf7 proteins are components of endosomal sorting complex required for transport III (ESCRT-III), which is composed of Vps20, Snf7, Vps24 and Vps2. The complex is involved in many cellular processes including cytokinesis, regulating membrane structures by forming a spiral coild-coil structure of Snf7 in membrane of endosome or plasma membrane (Henne et al., 2011; Schuh and Audhya, 2014) (Hurley and Hanson, 2010); McCullough, 2018 #102).

Especially in the endo-lysosomal pathway, ESCRT-III generates multivesicular body (MVB) where cargo proteins from endosomal membrane are stuck. Since endo-lysosomal pathway is deeply involved in cell survival and viability, dysfunction of ESCRT-III complex can affect the neuronal survival. Supporting this concept, there are some reports that dysfunction of ESCRT-III is involved in neurodegeneration. For examples, mutations in CHMP2B, a homolog of Vps2, is implicated in neurodegenerative diseases such as Alzheimer's diseases, frontotemporal dementia and amyotrophic lateral sclerosis (Cox et al., 2010; Hooli et al., 2014; Skibinski et al., 2005). A mouse line that mimic one of the mutations which makes a truncated form of CHMP2B, showed age-dependent social impairments (Gascon et al., 2014). In addition to that, knock-down of *Snf7-2*, a homolog of *Snf7-3*, caused autophagosome accumulation and neurodegeneration (Lee et al., 2007).

Although it is not well-known if Snf7 or ESCRT-III has a role in neurodevelopmental disorders, it seems that they have important roles in regulating neuronal developmental processes. Previously, my colleague studied the function of Snf7 in cortical neurons (Lee et al., 2007). According to her, in developing neuronal cultures, the expression of *Snf7-3* was highest on DIV 6, when the dendrite development is vigorous (Figure 12A). Then, she applied siRNA targeted to *Snf7-2* or *Snf7-3* to reduce the expression of the genes in neuron cultures. Interestingly, the knock-down of *Snf7-3* increased the length or branching of dendrites, while the knock-down of *Snf7-2* caused opposite phenotypes (Figure 12B). In addition to that, a drosophila homolog of *Snf7*, *Shrub*

promotes dendritic pruning during development, as deficiency of *Shrub* resulted in increased growth and branching of dendrites (Loncle et al., 2015; Sweeney et al., 2006). Since altered structural connectivity of nervous systems is implicated in neurodevelopmental disorders, I became interested in the protein and thought that it might be implicated in (Beare et al., 2017; Konrad and Eickhoff, 2010). Supporting the idea, a genetic study of human patients indicated that (SNPs) in *CHMP7*, a homologue of *Snf7*, may be involved in ADHD (Neale et al., 2010).
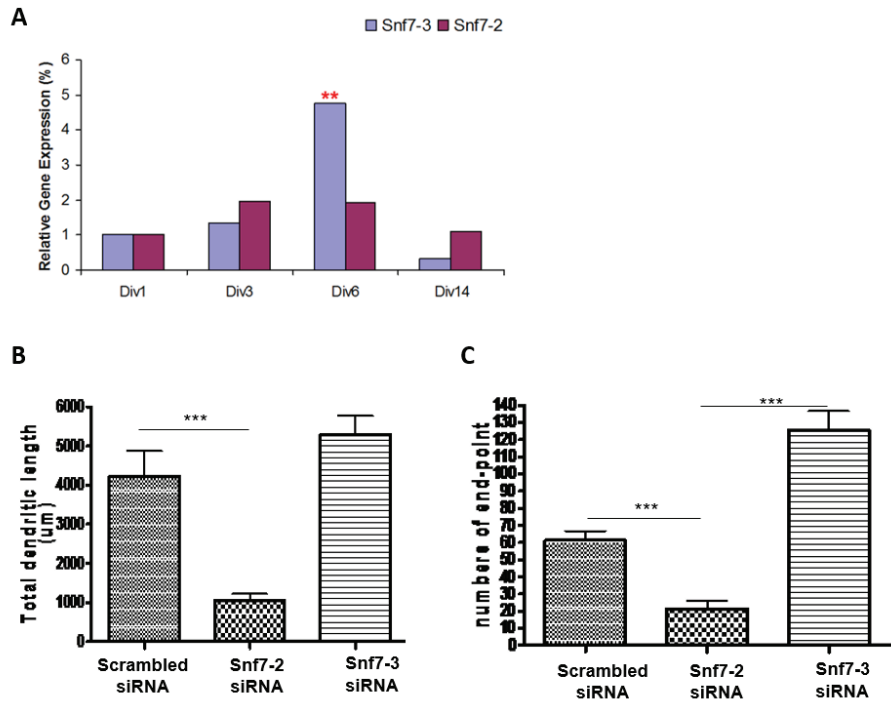
Figure 12. Differential role of Snf7-2 and *Snf7-3* in dendritic developments

(A) Increased expression of *Snf7-3* in cortical culture neurons on DIV6 when dendritic developments are vigorous, compared with other time points.

(B, C) Knock-down *of Snf7-2* significantly decreased total dendritic length and branching, while knock-down of *Snf7-3* causing opposite phenotypes.

(in collaboration with Dr. Jin-A Lee)

As implicated in the name of ADHD, the main symptoms of ADHD are inattention and hyperactivity. In most cases, impulsivity is also followed. Similarly, with ASDs, the prevalence of ADHD has been increased gradually during last decades and it is estimated to be 5.29% to 7.1% in children and adolescents (Fayyad et al., 2007). While medications such as amphetamine and methylprenidate, are used for treatment of ADHD, they can cause some side effects like sleep disorders or social withdrawal and the drugs are only partially effective to some patients (Punja et al., 2016).

To address if dysfunction of *Snf7-3* is implicated in phenotypes related with neurodevelopmental disorders, I generated two lines of *Snf7-3* deficient mouse. One is mouse line is like conventional KO in which the expression of *Snf7-3* is transcriptionally inhibited in all cells, while another is conditional KO in which *Snf7-3* is deleted in forebrain excitatory neurons. Both KO mouse lines showed hyperactivity and conditional KO mice displayed impaired object location memory, while the phenotypes disappeared when the mice became about 6 months old. Interestingly, the frequency of spontaneous excitatory transmission was elevated in hippocampus of the KO mice, suggesting altered E/I balance.

EXPERIMENTAL PROCEDURES

Animals

An embryonic stem cell line from European Conditional Mouse Mutagenesis Program (EUCOMM), in which a cassette, named as promotorless cassette, was inserted in front of exon 2 of *Snf7-3* gene (Figure 13A). This cassette contains polyadenylation sequence (pA), so the transcription of *Snf7-3* is inhibited. Thus, I used this for a mouse line that mimic conventional KO in which *Snf7-3* is not expressed in all cells. In addition to that, exon 2 of *Snf7-3* is flanked by loxP sites, which is recognized by Cre recombinase, so exon2 can be deleted under existence of Cre. In that case, the open reading frame of *Snf7-3* is changed and a stop codon is made in the very early position of the protein coding sequence. Thus after removing the promoterless cassette which is flanked by FRT sequences, the expression of *Snf7-3* is dependent on Cre recombinase.

The embryonic stem cell (ES cell) line was sent to a company, and injected to a mouse blastocyst. After implanting the blastocyst in a foster mouse, chimera mice were born. Newly born mice from the chimera mice was genotyped. These mice contained the promotorless cassette in their genome, so they were used for conventional KO line. For the conditional KO line, I mated the mice with a mouse line that express Cre recombinase only in Ca 2+/calmodulin-dependent protein kinase II α (CaMKIIα) neurons, which is a marker for excitatory forebrain neurons, so *Snf7-3* is not expressed only in the CaMKIIα neurons. Mice with a genotype of *Snf7-3* fl/fl; CaMKIIa-Cre +/- were used as conditional KO and littermate mice with a genotype of *Snf7-3* fl/fl; CaMKIIa-Cre -/- were used as WT controls (Figure 13B).

8 to 24 weeks or over than 25 weeks old mice were used for following experiments. Food and water were provided *ad libitum* and all the mice were kept on a 12 h light/dark cycle. All the experimental procedures were done during the light phase of the cycle. The Institutional Animal Care and Use Committee of Seoul National University approved the animal care and experiments.

56
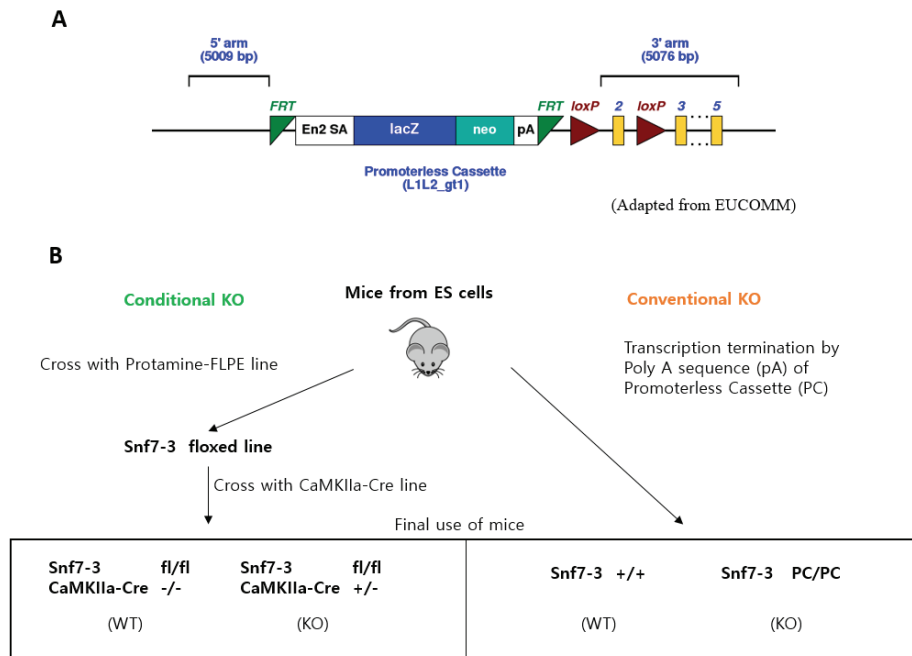
Figure 13. Generation of conventional and conditional *Snf7-3* KO lines

(A) Construction of *Snf7-3* gene area in a ES cell line from EUCOMM, which is designed to restrict the expression of *Snf7-3* by poly A sequence (pA) and with a potential to be used as conditional KO. (B) Generation of conventional and conditional KO mice. For conventional KO, pA sequence was maintained to block the transcription of *Snf7-3*. For conditional KO, the mice generated from ES cells were mated with protamine-FLPE line to remove pA sequence of PC. Then, to delete *Snf7-3* only in excitatory neurons of brain, the mice were mated with CaMKIIa-Cre mice to remove exon 2 making stop codon.

qRT-PCR

After anesthetization with isoflurane, hippocampi were extracted and grinded. Total RNA was separated by TRIZOL (Invitrogen). mRNA was reverse-transcribed using the poly-A primer and Superscript III (Invitrogen). qRT-PCR was performed in triplicate using ExTaqII SYBR Green Master Mix (Takara) in ABI7300 (Applied Biosystems) system. The sense primer (5' CAACACGGAGGTCTTACGGAA 3') was designed to detect exon 2 area of *Snf7-3* gene, while the anti-sense primer (5' GGCAAACTGAACCCTTTGAGAAA 3') was designed to detect exon 3 area. Cycling conditions were 95 °C for 30 s, followed by 40 cycles of 95 °C for 15 s, 60 °C for 20s and 72 °C 31 s. GAPDH was used as an internal control.

Behavioral Tests

Open-field test

A mouse was placed in the middle of a square white plexiglass box (40 × 40 × 40 cm) under dim light. The movement of the mouse and location in the box was tracked using a tracking program (EthoVision 9.0, Nodulus) for 20 min. The center was defined as the middle area that occupied 1/2 of the total area. 30 min before the test, L838,417 or vehicle was injected and experimenters were blinded to the genotypes and identity of injected drugs.

Elevated zero maze (EZM) test

A round-shaped (inner diameter: 50 cm, outer diameter: 60 cm) maze which is made of white Plexiglass and elevated 40 cm from the floor, was used. The maze was composed of 4 arms, 2 of open arms and 2 of closed arms with 20 cm walls on both sides. A mouse was placed on the center of one of closed arm of the maze, and the movement of the mouse was tracked for 5 min by using a tracking program (EthoVision 9.0, Nodulus), under bright light. If a mouse fell onto the floor, the mouse was excluded from the analysis. 30 min before the test, L838,417 or vehicle was injected and experimenters were blinded to the genotypes and identity of injected drugs.

Object location memory test

Mice were handled for 3 min on 4 consecutive days and then placed in a square box for 15 min on 2 consecutive days for habituation. The box has one transparent side and three white opaque sides, and opposite side of the transparent side have a visual cue. After the habituation, on conditioning day, two objects of same shape were placed sequentially in front of the opposite side of the transparent side. Mice explored the objects for 10 min. On next day (test day), one of the object was placed in front of the transparent side while the position of the other object was not changed. Mice explored the objects for 5 min and the ratio of time spent for investigating the moved object was calculated. If a mouse investigated the objects less than 10 secs or 2 secs, during conditioning and test respectively, the mouse was excluded for data. In addition, if a mouse investigated one object 3 times or more than the other object, the mouse was also excluded for data.

Three-chamber test

A three-chamber apparatus was made up of successive three chambers with a door between the faced two chambers (two outer chambers: 20 x 15 x 25 cm and an inner chamber: 20 x 10 x 25 cm). Stranger mice were habituated in a metal-wired cage placed in the outer chamber for 10 min on 4 consecutive days. *Shank2* KO mice and their littermate WT mice (test mice) were also habituated in the apparatus with the doors open on two consecutive days and they had not met with the stranger mice. 24 hours after the habituation, the test mouse was placed in the inner chamber with the doors open. After 10 min, the test mouse was guided to the inner chamber and the doors were closed. A wired cup with the stranger mouse (stranger) and a wired cup with yellow block (object) were introduced into each of the outer chamber, and then the doors were opened to test sociability. The movement of the test mouse was tracked for 10 min with a tracking program (EthoVision 9.0, Nodulus). 30 min before the test, L838,417 or vehicle was injected and experimenters were blinded to the genotypes and identity of injected drugs. Experimenters were blinded to the genotypes and identity of injected drugs.

Morris water maze (MWM) test

Mice were handled for 3 min on 4 consecutive days before performing the test. During training session, a mouse was placed into a white opaque water-filled (22–23 °C) tank (140 cm diameter, 100 cm height) placed in a room with multiple spatial cues under dim light. The tank was divided into 4 virtual fan-shaped quadrants, which target quadrant (TQ), opposite quadrant (OQ), adherent quadrant 1 (AQ1) and adherent quadrant 2 (AQ2). In a fixed location of TQ, a 10 cm diameter-platform was placed. On the training days, mice were pseudo-randomly released at the edge of the maze facing the inner wall of the tank and trained to reach the platform for 60 s. If the mice failed to reach the platform for 60 s, they were guided to the platform and maintained on the platform for 10 s. When the mice successfully reached the platform and stayed on the platform for more than 1 s, mice were rescued from the maze after 10 s. Mice were trained with 4 trials per day to be released at all the quadrants and the trial interval was 2 min. The day after the final day of 5 to 7 days of training, a probe test was performed. In the probe test, the platform was removed and a mouse was released at the center of the pool. The mouse was tracked for 60 s with a tracking program (EthoVision 9.0, Nodulus) and, mean distance from the platform, the number of platform location crossing and time spent in each quadrant were analyzed. Experimenters were blinded to the genotypes and identity of injected drugs.

Contextual fear conditioning

Mice were handled for 3 min on 4 consecutive days before the conditioning. After the handling, a mouse was placed in a conditioning chamber (Coulbourn instruments) for 210 secs and two electrical foot shocks (2 secs, 0.6 mA) were delivered at 150 secs and 180 secs respectively. Freezing level was analyzed by Freeze Frame program (Coulbourn instruments) before the first shock. After 24 hours, the mouse was returned to the chamber for 180 secs and freezing level was analyzed.

Electrophysiology

Mice were anesthetized with isoflurane and hippocampus or medial prefrontal cortex (mPFC) was extracted. 300um thick-slices were prepared using a vibratome (VT1200S;Leica) in ice-cold

N-methyl-D-glucamine (NMDG) solution (93 mM NMDG, 2.5 mM KCl, 1.2 mM NaH2PO4, 30 mM NaHCO3, 20 mM HEPES, 25 mM Glucose, 5 mM sodium ascorbate, 2 mM Thiourea, 3 mM sodium pyruvate, 10 mM MgSO4, 0.5 mM CaCl2) and recovered in the solution at 32 ~ 34℃. After 10min, the slices were transferred to artificial cerebrospinal fluid (ACSF) (124 mM NaCl, 2.5 mM KCl, 1 mM NaH2PO4, 25 mM NaHCO3, 10 mM glucose, 2 mM CaCl2, and 2 mM MgSO4) at room temperature and maintained for at least 1hr before the experiment. After recovery, the slices were placed in a recording chamber maintained at 30℃ and constantly perfused with oxygenated ACSF at a rate of 1ml/min.

The recording pipettes (3 ~ 5 MΩ) were filled with an internal solution containing 145mM K-gluconate, 5mM NaCl, 10mM HEPES, 1mM MgCl2, 0.2mM EGTA, 2mM MgATP, and 0.1mM Na3GTP (280 ~ 300 mOsm, adjust to pH 7.2 with KOH) with 0.2% biocytin. Picrotoxin (100 μM) and Tetrodotoxin (1 μM) were added to the ACSF to block the GABA-R-mediated currents and sodium channel mediated currents.

Pyramidal cells were selected by manually and voltage-clamped at -70 mV using an Axopatch 200B (Molecular Devices). After at least 5 min for complete diffusion of internal solution throughout the neuron, spontaneous postsynaptic currents are recorded during 5 min. This electrophysiological data was analyzed by MiniAnalysis program (Synaptosoft). Only neurons with a change of access resistance less than 20% were included in the analysis.

Dendrite analysis

Recording pipettes were filled with internal solution containing 2 mg/ml biocytin (pH 7.2 with KOH, 280–290 mOsm). After electrophysiological recordings, the brain slices were fixed with 4% paraformaldehyde. The fixed slices were then washed for 1 h three times with PBS and blocked with 5% goat serum and 0.2% Triton X-100 in PBS for 1 h at room temperature. For staining, the slices were incubated overnight at 4 ºC in streptavidin and Alexa Fluor® 488 conjugate (Life Technologies) at 1:2000 in the blocking solution. The slices were then washed for 1 h three times with PBS and mounted with 50 % glycerol on slide glasses. In the biocytin injected neuron, dendrites were imaged using a confocal microscopy (Leica, TCS SP8) with Z stacks and the Z

stack images were reconstructed to generate a 3D image of the biocytin injected neuron using a IMARIS software (Bitplane). Using the software, Sholl analysis was performed and the length or branching of each dendrite was analyzed.

Statistics

For the Morris water maze, the one-way ANOVA (analysis of variance) was performed to examine whether the mice spent significantly more time in the target quadrant than in the other three quadrants. For the three-chamber test and contextual fear memory test, two-way ANOVA was performed to evaluate the effects of genotype x target or genotype x time respectively. When two groups were compared, the unpaired two-tailed t-test was used. All data are represented as mean ± SEM and the statistical analyses were performed with Graphpad 5.0 software. Sample sizes including animal numbers were chosen to ensure adequate statistical power comparable to previously published papers. Data distribution of experiments was assumed to be normal.

RESULTS

Confirm of *Snf7-3* KO

I generated conventional and conditional *Snf7-3* KO lines, and I checked if *Snf7-3* is really not expressed in the KO mice as we expected. To confirm if the *Snf7-3* mRNA is not expressed in the conventional KO mice, I performed qRT-PCR in hippocampus and *Snf7-3* was barely expressed in the KO mice compared to WT littermates (Figure 14A). I also performed the same qRT-PCR in the conditional KO mice, and in this case the *Snf7-3* expression of KO mice was about half of that of WT littermates, which is concomitant with the feature of conditional KO (Figure 14B). I also performed western blot analysis to check if *Snf7-3* protein is not expressed, but the antibody quality for *Snf7-3* was not good, so I could not compare the *Snf7-3* protein level (data not shown).
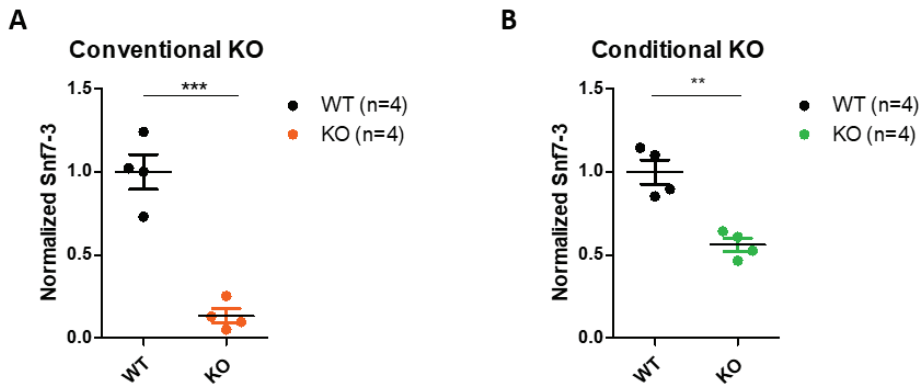
Figure 14. Reduced expression of *Snf7-3* in generated KO lines

(A) Decreased *Snf7-3* mRNA expression in the hippocampus of *Snf7-3* conventional KO mice (WT: n = 4, KO: n = 4, unpaired t-test ***$P < 0.001$). (B) Decreased *Snf7-3* mRNA expression in the hippocampus of *Snf7-3* conventional KO mice (WT: n = 4, KO: n = 4, unpaired t-test **$P < 0.01$). Since hippocampus consists of not only CaMKIIa neurons, but also other cells such as interneurons or glial cells, the expression of *Snf7-3* in hippocampus was not totally blocked.

Hyperactivity and a mild cognitive deficit of *Snf7-3* KO mice (8 to 24 weeks old)

Based on my colleague's data (Figure 12) showing that *Snf7-3* regulates the growth and branching of dendrites during developing neurons, I performed behavioral experiments which are involved in the symptoms of neurodevelopmental disorders, such as locomotion activity, emotional status and cognitive deficits.

At first, I addressed behavioral phenotypes of *Snf7-3* KO mice of 8 to 24 weeks, which is generally used age for behavioral experiments. I examined locomotive activity and anxiety of both conventional and conditional *Snf7-3* KO lines in open-field test and found that both KO mice moved much more distance in the open-field box compared to WT littermates (Figure 15A, D). Time duration in center area was comparable between KO and WT mice. Similarly, in elevated-zero maze test, time duration in open area of KO mice was not significantly different from that of WT littermates, suggesting that anxiety is not affected by the *Snf7-3* KO (Figure 15B, E). Because the hyperactivity is a primary symptom of ADHD, this suggests a relationship of *Snf7-3* with ADHD.

Since ASD is one of the most popular neurodevelopmental disorder, which is deeply related with social behaviors, the sociability and social recognition ability of *Snf7-3* KO mice was examined in three-chamber test. However, unlike the case of *Shank2* KO mice, both conventional and conditional KO mice showed normal social behaviors compared to WT littermates (Figure 15C, F).
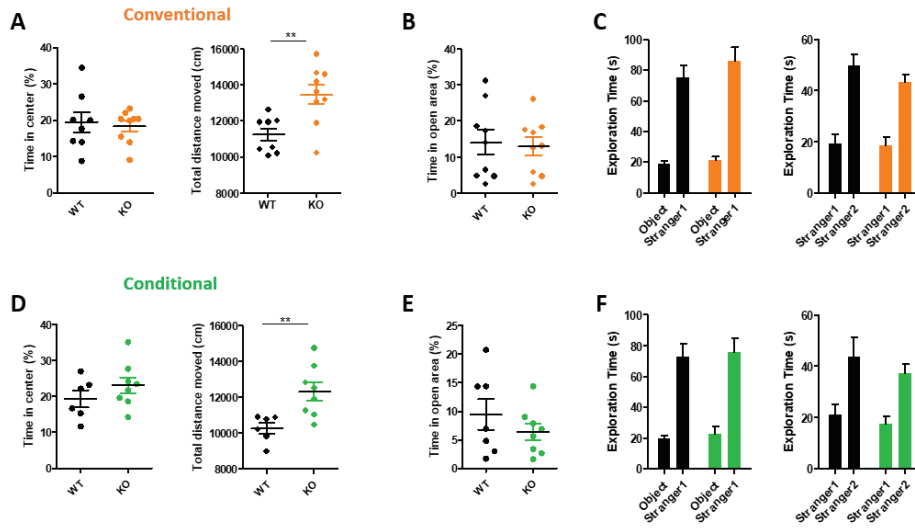
Figure 15. Locomotion, anxiety and social behaviors of 8 to 24 weeks old *Snf7-3* KO mice

(A, D) Increased locomotion activity with normal anxiety of *Snf7-3* conventional and conditional KO mice in the open-field test (Conventional, WT: n = 8, KO: n = 9, unpaired t-test **P < 0.01; Conditional, WT: n = 6, KO: n = 8, unpaired t-test **P < 0.01). (B, E) No significant change in anxiety in *Snf7-3* conventional and conditional KO mice in elevated zero maze (Conventional, WT: n = 8, KO: n = 9, unpaired t-test; Conditional, WT: n = 6, KO: n = 8, unpaired t-test). (C, F) No significant change in sociability (left panel) and social recognition (right panel) in *Snf7-3* conventional and conditional KO mice in three-chamber test (Conventional, WT: n = 8, KO: n = 9, two-way ANOVA, genotype x target; Conditional, WT: n = 6, KO: n = 8, two-way ANOVA, genotype x target).

Intellectual disabilities such as learning and memory deficits are frequently accompanied in the neurodevelopmental conditions. Thus I investigated learning and memory abilities in the KO mice. At first, I performed object location memory test that examine a kind of spatial memory of mice. In the test, conventional KO mice showed comparable exploration for the moved object with WT littermates, indicating that they could memorize the location of objects well (Figure 16A). However, conditional KO mice showed a little bit, but significantly impaired location memory compared to WT littermates, suggesting a mild cognitive deficit in conditional KO mice (Figure 16D). Furthermore, I also performed Morris-water maze task, another spatial memory test. In the test, both conventional and conditional KO mice learned and memorized the position of a platform well as much as WT littermates (Figure 16C, E). Finally, the contextual fear memory of the KO mice was evaluated, which is one of the most common form of memory tested in laboratories, and there was no significant difference in the contextual fear memory between WT and KO mice (Figure 16D, F).
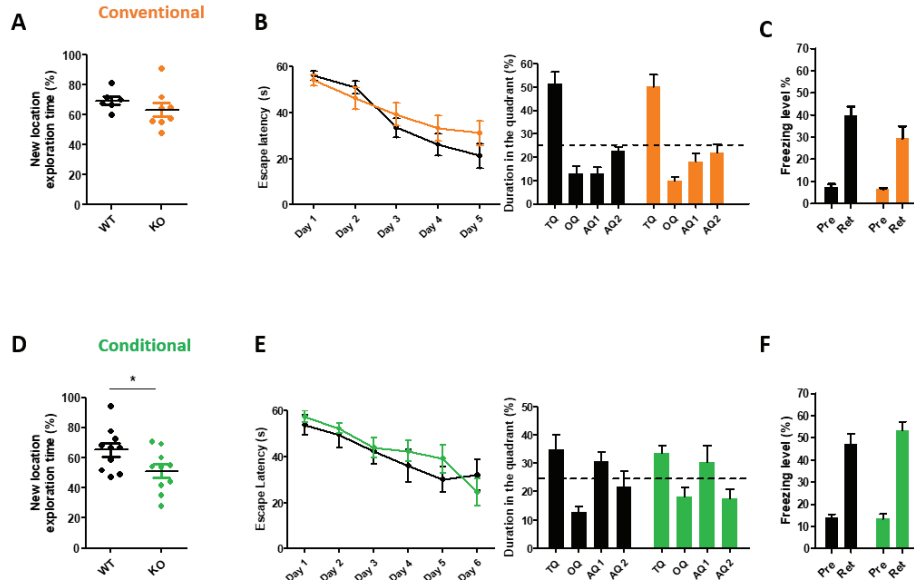
Figure 16. Hippocampus dependent spatial and contextual fear memories of 8 to 24 weeks old *Snf7-3* KO mice

(A) No significant change in object location memory of *Snf7-3* conventional KO mice (WT: n = 6, KO: n = 8, unpaired t-test). (D) Impaired object location memory of *Snf7-3* conditional KO mice (WT: n = 11, KO: n = 10, unpaired t-test *P < 0.05) (B, E) Learning curve (left panel) and probe test (right panel) of *Snf7-3* conventional and conditional KO in Morris-water maze. The learning ability or spatial memory of *Snf7-3* KO mice were comparable to those of WT mice (Conventional, WT: n = 8, KO: n = 9; Conditional, WT: n = 6, KO: n = 8). (C, F) No significant change in contextual fear memory of *Snf7-3* conventional and conditional KO (Conventional, WT: n = 8, KO: n = 9, two-way ANOVA, genotype x time; Conditional, WT: n = 6, KO: n = 8, two-way ANOVA, genotype x time). Pre: before conditioning, Ret: during retrieval (after conditioning)

Normal locomotion activity in relatively old *Snf7-3* KO mice (more than 25 weeks old)

Neurodevelopmental disorders are prominently studied in early ages like childhood, and sometimes the symptoms get better as the individual grows (Bishop and Rutter, 2009). To address if the abnormal behavioral features were also reproduced in the relatively old ages, I performed the behavioral tests of above again with different group of mice. Interestingly, the hyperactivity of KO mice in the open-field test was not shown. Anxiety like behaviors in elevated-zero maze was comparable between WT and KO mice, as in the relatively young mouse groups (Figure 17B, E). The locomotion activity of them was similar with that of WT littermates in both conventional and conditional KO lines (Figure 17A, D). The total distance moved in WT littermate mice was not that different from that of relatively young 8 to 24 weeks old WT mice. In addition to that, object location memory was also comparable between KO and WT mice, even in the conditional KO lines (Figure 18A, D). These indicate that hyperactivity and cognitive deficit of *Snf7-3* KO mice have disappeared as the mice growing.

Social recognition of the relatively old KO mice tended to be impaired slightly, supporting the previous reports that ESCRTIII complex is involved in social behaviors at old ages (Gascon et al., 2014) (Figure 17C, F). Contextual fear memory and spatial memory in Morris-water maze were not significantly impaired, similarly to the results of relatively young 8 to 24 weeks old mice (Figure 18B, C, E, F).
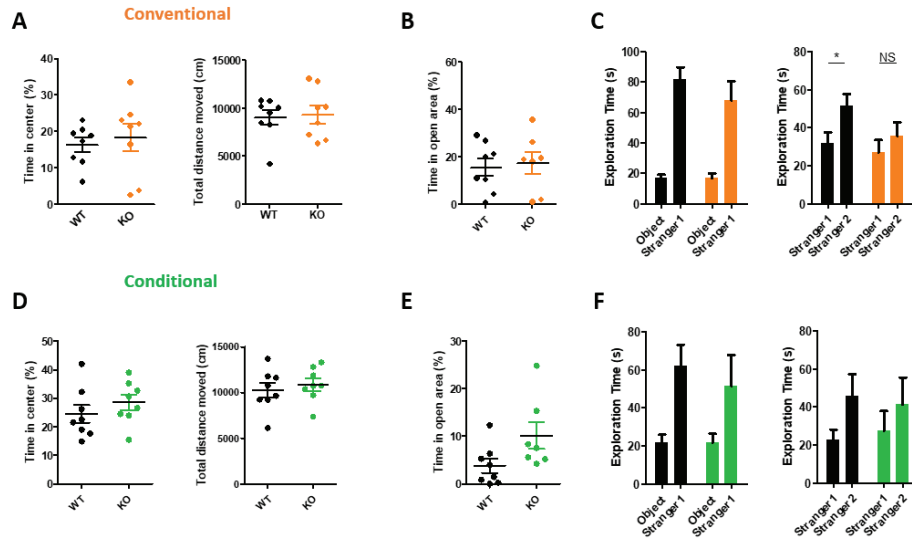
Figure 17. Locomotion, anxiety and social behaviors of more than 25 weeks old *Snf7-3* KO mice

(A, D) No change in locomotion activity and anxiety of *Snf7-3* conventional and conditional KO mice in the open-field test (Conventional, WT: n = 8, KO: n = 8, unpaired t-test; Conditional, WT: n = 8, KO: n = 8, unpaired t-test). (B, E) No significant change in anxiety in *Snf7-3* conventional and conditional KO mice in elevated zero maze (Conventional, WT: n = 8, KO: n = 8, unpaired t-test; Conditional, WT: n = 8, KO: n = 8, unpaired t-test). (C, F) No significant change in sociability (left panel) in *Snf7-3* conventional and conditional KO mice, while the social recognition (right panel) of *Snf7-3* conventional KO mice was impaired compared to WT littermates (Conventional, WT: n = 8, KO: n = 8, two-way ANOVA, genotype x target, paired t-test *P < 0.05). NS, not significant.
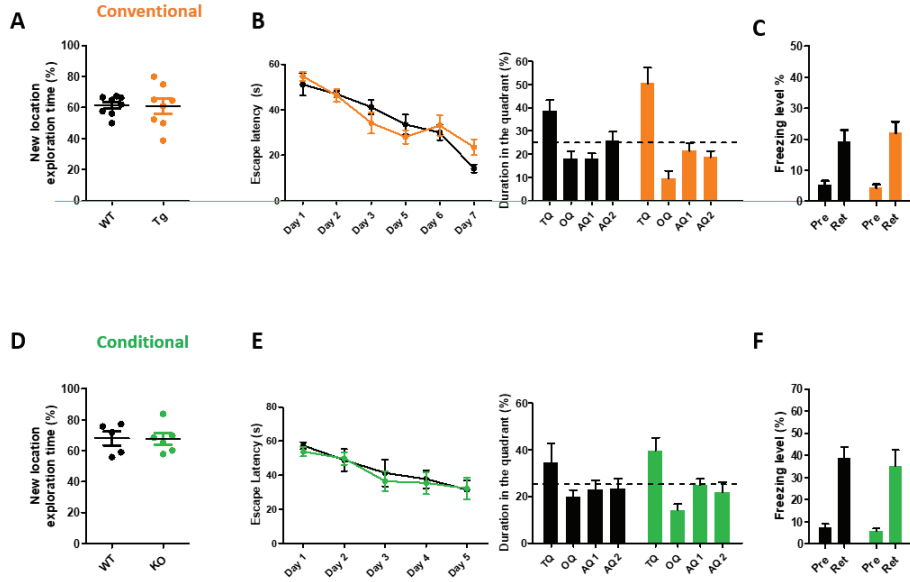
Figure 18. Hippocampus dependent spatial and contextual fear memories of more than 25 weeks old *Snf7-3* KO mice

(A, D) No significant change in object location memory of *Snf7-3* conventional and conditional KO mice (WT: n = 8, KO: n = 8, unpaired t-test; WT: n = 5, KO: n = 6, unpaired t-test) (B, E) Learning curve (left panel) and probe test (right panel) of *Snf7-3* conventional and conditional KO in Morris-water maze. The learning ability or spatial memory of *Snf7-3* KO mice were comparable to those of WT mice (Conventional, WT: n = 8, KO: n = 8; Conditional, WT: n = 8, KO: n = 8). (C, F) No significant change in contextual fear memory of *Snf7-3* conventional and conditional KO (Conventional, WT: n = 8, KO: n = 8, two-way ANOVA, genotype x time; Conditional, WT: n = 8, KO: n = 8, two-way ANOVA, genotype x time). Pre: before conditioning, Ret: during retrieval (after conditioning)

Dendrite growth and complexity in *Snf7-3* KO mice

Previously, the knock-down *Snf7-3* caused increased dendrite complexity in neuronal culture, so I examined if the dendrite growth or morphology is changed in the *Snf7-3* KO mice. Among lots of brain region, I chose medial prefrontal cortex (mPFC) and hippocampus. mPFC is known to be involved in neurodevelopmental disorders, regulating cognitive functions like planning, and dysregulation of connectivity or activity in the area is associated with cognitive dysfunction in ADHD (Bos et al., 2017; Yabuki et al., 2014). Hippocampus is also deeply involved in object location memory and represent abnormal features of neurodevelopmental disorders in patients and animal models (Lim et al., 2017; Plessen et al., 2006; Won et al., 2012).

The length and number of dendrites are analyzed in biocytin injected neurons in each brain region of conditional KO mice (Figure 19A, C). However, total length or number of dendrites were not significantly different between KO and WT mice, even if the average length of dendrites were tended to be longer in KO mice than WT littermates. In spite of the results, in the Sholl analysis, there are a mild tendency of increased branching of dendrites at length about100 to 200 µm, in mPFC (Figure 19B, C), supporting the previous knock-down results. The analysis was performed with adult mice over 8 weeks old, but dendritic branching is vigorous between from embryonic day 15 to postnatal day 21 (Koleske, 2013). Thus in juvenile or pups, the dendrite growth and branching of KO may be more exaggerated than those of WT littermates.
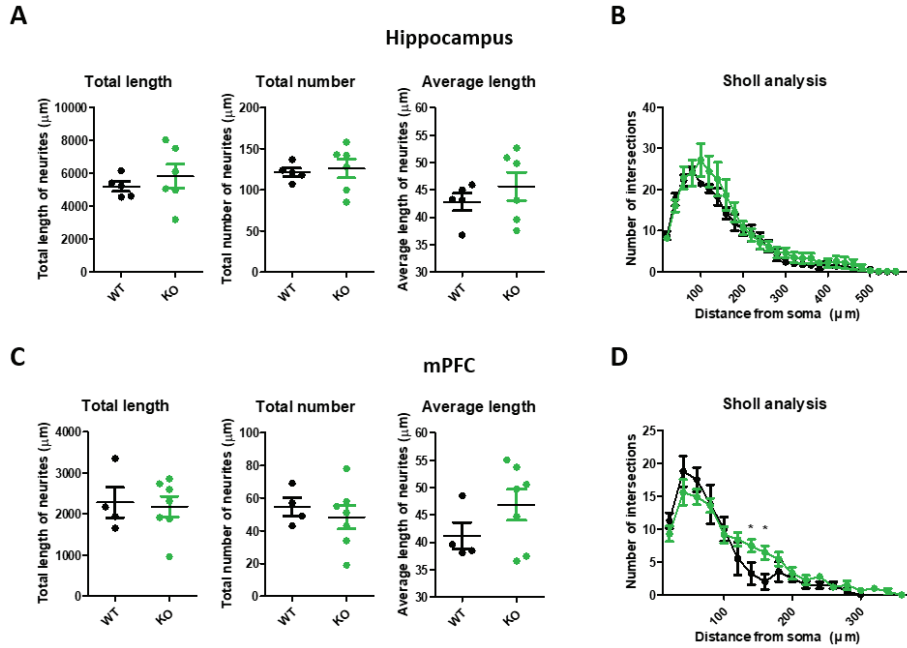
Figure 19. Dendrite growth and complexity in the hippocampus and mPFC of conditional *Snf7-3* KO mice

(A, C) No significant change in the total length, total number and average length of dendrites in the hippocampus or mPFC of *Snf7-3* conditional KO mice (Hippocampus, WT: n = 5, KO: n = 6, unpaired t-test; mPFC, WT: n = 4, KO: n = 7, unpaired t-test). (B, D) Sholl analysis of neurons in hippocampus or mPFC of *Snf7-3* conditional KO mice. There is a slight increase of intersections in neurons of mPFC (Hippocampus, WT: n = 5, KO: n = 6, unpaired t-test; mPFC, WT: n = 4, KO: n = 7, unpaired t-test *P < 0.05).

(in collaboration with June hyun Jeong)

Increased spontaneous excitatory neurotransmission in *Snf7-3* KO mice

Abnormal neurotransmission and altered E/I balance are frequently reproduced phenotypes in animal models of neurodevelopmental disorders. Thus spontaneous excitatory neurotransmission was recorded in the hippocampus and mPFC of *Snf7-3* conditional KO mice, using whole cell voltage-clamp technique. Interestingly, the frequency of mEPSC was significantly increased in hippocampus, while the amplitude was comparable to WT littermates (Figure 20). I did not investigate mIPSC yet, but the increased mEPSC suggests the possibility of alteration in E/I ratio.
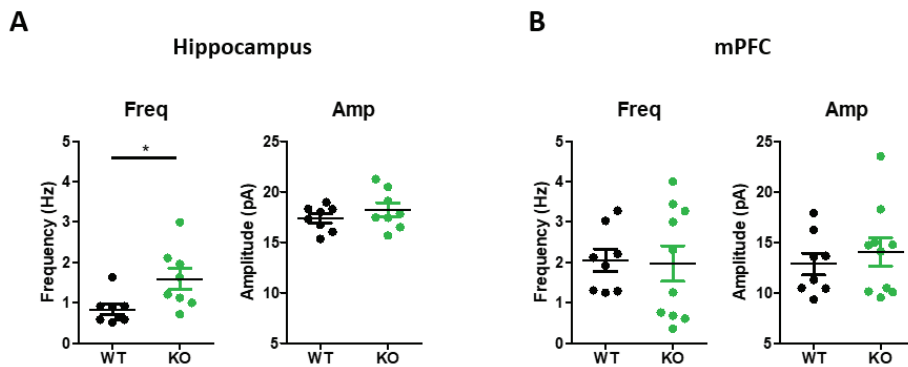
Figure 20. Spontaneous mEPSC frequency and amplitude in the hippocampus and mPFC of *Snf7-3* conditional KO mice

(A) Increased frequency of mEPSC in neurons in hippocampus of *Snf7-3* conditional KO mice (WT: n = 8, KO: n = 8, unpaired t-test *P < 0.05). mESPC amplitude was not changed in hippocampus. (B) No change in frequency and amplitude in neurons in mPFC of *Snf7-3* conditional KO mice (WT: n = 8, KO: n = 10, unpaired t-test).

(in collaboration with Dr. Su-Eon Sim & Jisu Lee)

Discussion

In the present study, I examined the role of *Snf7-3* in relation with neurodevelopmental disorders based on previous results of *Snf7-3* knock-down showing that reduced *Snf7-3* could result in abnormal increased dendrite growth and branching. For that purpose, I generated conventional and conditional *Snf7-3* KO mouse lines from ES cells and investigated behavioral and physiological phenotypes of the mice. Interestingly, both conventional and conditional KO mice showed increased locomotion activity, and conditional KO mice showed object location memory deficit. The hyperactivity and cognitive deficit disappeared in the relatively old group of mice, supporting the idea that these behavioral phenotypes are implicated in neurodevelopmental disorder. In addition to that, the excitatory neurotransmission was increased in the hippocampus of conditional KO mice, suggesting the possibility of alteration in E/I balance. Taken together, these data suggest that dysfunction of *Snf7-3* may be attributed to the pathways of neurodevelopmental disorders such as ADHD.

Involvement of ESCRTIII in neurodevelopmental processes and ADHD

Role ESCRTIII complex or endo-lysosomal pathway in neurodevelopmental disorders is not well studied yet. However, there are evidences that ESCRTIII or homologues of Snf7 are important for pruning of dendrite during circuit maturation, indicating the they have roles in neurodevelopmental processes (Loncle et al., 2015; Sweeney et al., 2006). In addition, recently a group of researchers showed that a mutation in Vps15 gene which is crucial for endosomal pathway, perturbed neuronal migration during development (Gstrein et al., 2018), emphasizing the relationship between enso-lysomal pathway and neurodevelopmental processes.

Genetic studies of ADHD patients have assisted to understand the cellular and molecular pathways that affects the condition. Usually, mutations in genes implicated in monoamine neurotransmitter systems are frequently observed to be involved in ADHD (Li et al., 2014). Among the monoamines, dopamine is highly implicated in the disorder in genetic studies, and

dopamine function in striatum is directly involved with movement regulation. Since endo-lysosomal pathway regulates the degradation process of membrane receptor cargo, it can affect dopamine pathway regulating such as dopamine receptors. Supporting this, dopamine D2 receptor (D2R) is degraded through MVBs formatted by ESCRTIII complex (Rosciglione et al., 2014). Since loss of D2R causes hypoactivity (Yamaguchi et al., 1996), dysregulation of D2R caused by dysfunction of ESCRTIII complex may resulted in hyperactivity.

Differences between Snf7-2 and Snf7-3.

Snf7-2 and Snf7-3 share quite similar sequence and structure like coiled-coil domain, except a little difference in the C terminal tail. Both of them interact with Vps20 in ESCRTIII complex and generate a spiral structure on membrane. It is not certain why the similar proteins have different roles in regulating dendrite developments yet. However, there are some other clues that suggesting different roles of the two Snf7 proteins.

At first, express pattern of them is different. Absolute expression of Snf7-2 is much higher than that of Snf7-3 in mouse brain, and Snf7-3 is mostly expressed in kidney, while Snf7-2 is mostly expressed in CNS and placenta (Yue et al., 2014). In addition, when Snf7-3 was overexpressed in culture neurons, it seemed that actin cytoskeleton structures collapsed, while overexpression of Snf7-2 did not show the phenomena (data not shown). Furthermore, there are some reports that suggest the specific role of Snf7-3 in regulating checkpoint of cellular processes in human cell lines. According to the reports, SNF7-3 stabilizes microtubule attach to kinetochore during mitotic processes, and depletion of SNF7-3 exaggerated early cytokinesis (Carlton et al., 2012; Petsalaki et al., 2018). Based on the reports, Snf7-3 may regulate microtubule structures of dendrites which is critical for stability of them, differently from Snf7-2.

E/I balance and hyperactivity

E/I balance is perturbed in many cases ADHD and ASD with hyperactivity (Brennan and Arnsten, 2008; Naaijen et al., 2017). For example, children who suffer from ADHD, showed reduced GABA concentration in a MRI study (Edden et al., 2012). In addition, a group of researchers investigated hundreds of variants in glutamatergic or GABAergic genes known to be

related with ADHD, and they found that mutations in the gene sets have correlation with the severity of hyperactivity/impulsivity symptoms in ADHD patients (Naaijen et al., 2017). In the case of animal model, N-myc downstream-regulated gene 2 (NDRG2) deficient mouse with ADHD-like behaviors, showed increased glutamatergic transmission and increased amplitude of mEPSC with normal mIPSC (Li et al., 2017b). In the paper, injecting NDRG2 peptides could rescue the increased excitatory transmission and hyperactivity. Furthermore, deficiency of GABA transporter subtype 1 (GAT1) resulted in ADHD phenotypes including hyperactivity (Chen et al., 2015; Yang et al., 2013). There are not many reports that showing the rescue of hyperactivity by restoring E/I balance, but it seems that the correlation between E/I balance and hyperactivity is clearly exist and studying the relationship would contribute to develop treatments for ADHD.

CHAPTER IV

CONCLUSION

CONCLUSION

In this study, I have investigated behavioral and physiological phenotypes, and implicated molecular mechanisms in animal models of neurodevelopmental disorders such as ASD and ADHD.

In Chapter II, I focused on *Shank2* KO mice and compared two *Shank2* KO lines. Previously, mutations in SHANK2 gene are associated with ASD and intellectual disability in human patient studies (Berkel et al., 2010). In addition, two lines of *Shank2* knockout mice (*Shank2* KO e67 and e7) showed similar autistic-like behaviors, but different physiological phenotypes (Schmeisser et al., 2012; Won et al., 2012). In the present study, I compared the transcriptomes of *Shank2* KO and e7 KO mice using RNA sequencing and found that mRNA level of *Gabra2*, which encodes the α2 subunit of GABAA receptors, is significantly reduced only in *Shank2* KO e67 mice, while the expression was unchanged in *Shank2* KO e7 mice. Based on the finding, I showed that GABAergic neurotransmission is impaired in *Shank2* KO e67 mice and the spatial memory deficit in the KO mice could be ameliorated by elevating the GABAergic neurotransmission by L838,417. I discovered a novel mechanism underlining the memory deficit of an ASD mouse model, and the finding would be helpful to treat individuals with ASD as lots of them have intellectual disabilities and memory deficits.

L838,417 treatment did not affect the spatial memory deficit of *Shank2* KO e7 mice and social behaviors even in *Shank2* KO e67 mice. It is worth noting that ASD is genetically and behaviorally heterogeneous, and each individual patient with specific mutations in the same gene may have a different underlying molecular even for a similar symptom. Furthermore, different domains of symptoms may have distinct underlying mechanisms. The present study indicates the importance of the development of individualized treatment for in some cases of ASD.

In Chapter III, I studied the role of *Snf7-3*, which constitutes a spiral structure in ESCRTIII complex, in neurodevelopmental processes and disorders. Previously, my colleague showed that down-regulation of *Snf7-3* caused increased dendrite growth and branching during dendrite

developmental period in culture. I generated *Snf7-3* KO mice and the mice showed hyperactivity with a mild cognitive deficit. Furthermore, frequency of mEPSC was elevated in *Snf7-3* KO mice, indicating alteration of E/I balance in the KO mice. Taken together, I suggest a novel role of ESCRTIII complex and endo-lysosomal pathway in ADHD or other neurodevelopmental disorders.

However, there are still many aspects to be examined. Although hyperactivity is one of primary symptoms of ADHD, the patients are frequently characterized by impulsivity and attention deficits. To address these symptoms, other behavioral tests can be done, such as 5-choice serial reaction time task which estimates impulsivity and attention in animals. Furthermore, dendrite growth and branching of *Snf7-3* KO mice should be examined again in relatively young mice along with dendrite developmental period. Finally, it would be worth to investigate whether abnormal dendrite complexity have causal relationship with the hyperactivity.

The cost for treating neurodevelopmental disorders including ASDs and ADHD have been increased as the prevalence increasing. According to a report, the annual costs associated with ASD in the United States is estimated to about $250 billion (Buescher et al., 2014). Despite the huge amount of costs, there is no effective treatment for the disorders yet, because of the complex and dynamic characteristic of them. Thus multidirectional studies should be done dealing with various cases associated with neurodevelopmental disorders. My works with the *Shank2* KO and *Snf7-3* KO mice would contribute to understanding molecular and physiological mechanisms of the disorders.

Acknowledgements

References

Baker, S.A., Chen, L., Wilkins, A.D., Yu, P., Lichtarge, O., and Zoghbi, H.Y. (2013). An AT-hook domain in MeCP2 determines the clinical course of Rett syndrome and related disorders. Cell 152, 984-996.

Beare, R., Adamson, C., Bellgrove, M.A., Vilgis, V., Vance, A., Seal, M.L., and Silk, T.J. (2017). Altered structural connectivity in ADHD: a network based analysis. Brain Imaging and Behavior 11, 846-858.

Benarroch, E.E. (2007). GABAA receptor heterogeneity, function, and implications for epilepsy. Neurology 68, 612-614.

Berkel, S., Marshall, C.R., Weiss, B., Howe, J., Roeth, R., Moog, U., Endris, V., Roberts, W., Szatmari, P., Pinto, D., et al. (2010). Mutations in the SHANK2 synaptic scaffolding gene in autism spectrum disorder and mental retardation. Nature Genetics 42, 489-491.

Bishop, D., and Rutter, M. (2009). Neurodevelopmental Disorders: Conceptual Issues. In Rutter's Child and Adolescent Psychiatry: Fifth Edition, pp. 32-41.

Bos, D.J., Oranje, B., Achterberg, M., Vlaskamp, C., Ambrosino, S., de Reus, M.A., van den Heuvel, M.P., Rombouts, S.A.R.B., and Durston, S. (2017). Structural and functional connectivity in children and adolescents with and without attention deficit/hyperactivity disorder. Journal of Child Psychology and Psychiatry and Allied Disciplines 58, 810-818.

Braat, S., and Kooy, R.F. (2015). The GABAA Receptor as a Therapeutic Target for Neurodevelopmental Disorders. Neuron 86, 1119-1130.

Brennan, A.R., and Arnsten, A.F.T. (2008). Neuronal mechanisms underlying attention deficit hyperactivity disorder: The influence of arousal on prefrontal cortical function. In Annals of the New York Academy of Sciences, pp. 236-245.

Buescher, A.V.S., Cidav, Z., Knapp, M., and Mandell, D.S. (2014). Costs of autism spectrum disorders in the United Kingdom and the United States. JAMA Pediatrics 168, 721-728.

Buffington, S.A., Di Prisco, G.V., Auchtung, T.A., Ajami, N.J., Petrosino, J.F., and Costa-Mattioli, M. (2016). Microbial Reconstitution Reverses Maternal Diet-Induced Social and Synaptic Deficits in Offspring. Cell 165, 1762-1775.

Carlton, J.G., Caballe, A., Agromayor, M., Kloc, M., and Martin-Serrano, J. (2012). ESCRT-III governs the Aurora B-mediated abscission checkpoint through CHMP4C. Science 336, 220-225.

Chao, H.T., Chen, H., Samaco, R.C., Xue, M., Chahrour, M., Yoo, J., Neul, J.L., Gong, S., Lu, H.C., Heintz, N., et al. (2010). Dysfunction in GABA signalling mediates autism-like stereotypies and Rett syndrome phenotypes. Nature 468, 263-269.

Chen, L., Yang, X., Zhou, X., Wang, C., Gong, X., Chen, B., and Chen, Y. (2015). Hyperactivity and impaired attention in Gamma aminobutyric acid transporter subtype 1 gene knockout mice. Acta Neuropsychiatrica 27, 368-374.

Christensen, J., Grnøborg, T.K., Srøensen, M.J., Schendel, D., Parner, E.T., Pedersen, L.H., and Vestergaard, M. (2013). Prenatal valproate exposure and risk of autism spectrum disorders and childhood autism. JAMA - Journal of the American Medical Association 309, 1696-1703.

Cox, L.E., Ferraiuolo, L., Goodall, E.F., Heath, P.R., Higginbottom, A., Mortiboys, H., Hollinger, H.C., Hartley, J.A., Brockington, A., Burness, C.E., et al. (2010). Mutations in CHMP2B in lower motor neuron predominant amyotrophic lateral sclerosis (Schmeisser et al.). PLoS ONE 5.

Cui, Y., Costa, R.M., Murphy, G.G., Elgersma, Y., Zhu, Y., Gutmann, D.H., Parada, L.F., Mody, I., and Silva, A.J. (2008). Neurofibromin Regulation of ERK Signaling Modulates GABA Release and Learning. Cell 135, 549-560.

Dixon, C.I., Rosahl, T.W., and Stephens, D.N. (2008). Targeted deletion of the GABRA2 gene encoding α2-subunits of GABAA receptors facilitates performance of a conditioned emotional response, and abolishes anxiolytic effects of benzodiazepines and barbiturates. Pharmacology Biochemistry and Behavior 90, 1-8.

Edden, R.A.E., Crocetti, D., Zhu, H., Gilbert, D.L., and Mostofsky, S.H. (2012). Reduced GABA concentration in attention-deficit/hyperactivity disorder. Archives of General Psychiatry 69, 750-753.

Etherton, M.R., Blaiss, C.A., Powell, C.M., and Südhof, T.C. (2009). Mouse neurexin-1α deletion causes correlated electrophysiological and behavioral changes consistent with cognitive impairments. Proceedings of the National Academy of Sciences of the United States of America 106, 17998-18003.

Fatemi, S.H., Reutiman, T.J., Folsom, T.D., Rustan, O.G., Rooney, R.J., and Thuras, P.D. (2014). Downregulation of GABA$_A$receptor protein subunits α6, β2, δ, ε, γ2, θ, and ρ2 in superior frontal cortex of subjects with autism. Journal of Autism and Developmental Disorders 44, 1833-1845.

Fayyad, J., De Graaf, R., Kessler, R., Alonso, J., Angermeyer, M., Demyttenaere, K., De Girolamo, G., Haro, J.M., Karam, E.G., Lara, C., et al. (2007). Cross-national prevalence and correlates of adult attention-deficit hyperactivity disorder. British Journal of Psychiatry 190, 402-409.

Gascon, E., Lynch, K., Ruan, H., Almeida, S., Verheyden, J.M., Seeley, W.W., Dickson, D.W.,

Petrucelli, L., Sun, D., Jiao, J., et al. (2014). Alterations in microRNA-124 and AMPA receptors contribute to social behavioral deficits in frontotemporal dementia. Nature Medicine 20, 1444-1451.

Gkogkas, C.G., Khoutorsky, A., Ran, I., Rampakakis, E., Nevarko, T., Weatherill, D.B., Vasuta, C., Yee, S., Truitt, M., Dallaire, P., et al. (2013). Autism-related deficits via dysregulated eIF4E-dependent translational control. Nature 493, 371-377.

Gonzalez-Nunez, V. (2015). Role of gabra2, GABA$_A$receptor alpha-2 subunit, in CNS development. Biochemistry and Biophysics Reports 3, 190-201.

Govek, E.E., Newey, S.E., and Van Aelst, L. (2005). The role of the Rho GTPases in neuronal development. Genes and Development 19, 1-49.

Gunaydin, L.A., Grosenick, L., Finkelstein, J.C., Kauvar, I.V., Fenno, L.E., Adhikari, A., Lammel, S., Mirzabekov, J.J., Airan, R.D., Zalocusky, K.A., et al. (2014). Natural neural projection dynamics underlying social behavior. Cell 157, 1535-1551.

Han, S., Tai, C., Jones, C.J., Scheuer, T., and Catterall, W.A. (2014). Enhancement of inhibitory neurotransmission by GABAA receptors having α2,3-subunits ameliorates behavioral deficits in a mouse model of autism. Neuron 81, 1282-1289.

Han, S., Tai, C., Westenbroek, R.E., Yu, F.H., Cheah, C.S., Potter, G.B., Rubenstein, J.L., Scheuer, T., De La Iglesia, H.O., and Catterall, W.A. (2012). Autistic-like behaviour in Scn1a+-mice and rescue by enhanced GABA-mediated neurotransmission. Nature 489, 385-390.

Henne, W., Buchkovich, N., and Emr, S. (2011). The ESCRT Pathway. Developmental Cell 21, 77-91.

Hines, R.M., Wu, L., Hines, D.J., Steenland, H., Mansour, S., Dahlhaus, R., Singaraja, R.R., Cao, X., Sammler, E., Hormuzdi, S.G., et al. (2008). Synaptic imbalance, stereotypies, and impaired social interactions in mice with altered neuroligin 2 expression. Journal of Neuroscience 28, 6055-6067.

Hogart, A., Nagarajan, R.P., Patzel, K.A., Yasui, D.H., and LaSalle, J.M. (2007). 15q11-13 GABAA receptor genes are normally biallelically expressed in brain yet are subject to epigenetic dysregulation in autism-spectrum disorders. Human Molecular Genetics 16, 691-703.

Hooli, B.V., Kovacs-Vajna, Z.M., Mullin, K., Blumenthal, M.A., Mattheisen, M., Zhang, C., Lange, C., Mohapatra, G., Bertram, L., and Tanzi, R.E. (2014). Rare autosomal copy number variations in early-onset familial Alzheimer's disease. Molecular Psychiatry 19, 676-681.

Houbaert, X., Zhang, C.L., Gambino, F., Lepleux, M., Deshors, M., Normand, E., Levet, F., Ramos, M., Billuart, P., Chelly, J., et al. (2013). Target-specific vulnerability of excitatory synapses leads to deficits in associative memory in a model of intellectual disorder. Journal of Neuroscience 33, 13805-13819.

Hung, A.Y., Futai, K., Sala, C., Valtschanoff, J.G., Ryu, J., Woodworth, M.A., Kidd, F.L., Sung, C.C., Miyakawa, T., Bear, M.F., et al. (2008). Smaller dendritic spines, weaker synaptic transmission, but enhanced spatial learning in mice lacking Shank1. Journal of Neuroscience 28, 1697-1708.

Hurley, J.H., and Hanson, P.I. (2010). Membrane budding and scission by the ESCRT machinery: It's all in the neck. Nature Reviews Molecular Cell Biology 11, 556-566.

Kim, H., Lim, C.S., and Kaang, B.K. (2016). Neuronal mechanisms and circuits underlying repetitive behaviors in mouse models of autism spectrum disorder. Behavioral and Brain Functions 12.

Kim, Y.S., Leventhal, B.L., Koh, Y.J., Fombonne, E., Laska, E., Lim, E.C., Cheon, K.A., Kim, S.J., Kim, Y.K., Lee, H., et al. (2011). Prevalence of autism spectrum disorders in a total population sample. American Journal of Psychiatry 168, 904-912.

Koleske, A.J. (2013). Molecular mechanisms of dendrite stability. Nature Reviews Neuroscience 14, 536-550.

Konrad, K., and Eickhoff, S.B. (2010). Is the ADHD brain wired differently? A review on structural and functional connectivity in attention deficit hyperactivity disorder. Human Brain Mapping 31, 904-916.

Kroon, T., Sierksma, M.C., and Meredith, R.M. (2013). Investigating mechanisms underlying neurodevelopmental phenotypes of autistic and intellectual disability disorders: A perspective. Frontiers in Systems Neuroscience 7.

Leblond, C.S., Nava, C., Polge, A., Gauthier, J., Huguet, G., Lumbroso, S., Giuliano, F., Stordeur, C., Depienne, C., Mouzat, K., et al. (2014). Meta-analysis of SHANK Mutations in Autism Spectrum Disorders: A Gradient of Severity in Cognitive Impairments. PLoS Genetics 10.

Lee, E., Lee, J., and Kim, E. (2017). Excitation/Inhibition Imbalance in Animal Models of Autism Spectrum Disorders. Biological Psychiatry 81, 838-847.

Lee, J.A., Beigneux, A., Ahmad, S.T., Young, S.G., and Gao, F.B. (2007). ESCRT-III Dysfunction Causes Autophagosome Accumulation and Neurodegeneration. Current Biology 17, 1561-1567.

Lee, Y.S., Ehninger, D., Zhou, M., Oh, J.Y., Kang, M., Kwak, C., Ryu, H.H., Butz, D., Araki, T., Cai, Y., et al. (2014). Mechanism and treatment for learning and memory deficits in mouse models of Noonan syndrome. Nature Neuroscience 17, 1736-1743.

Li, Q., Han, Y., Dy, A.B.C., and Hagerman, R.J. (2017a). The gut microbiota and autism spectrum disorders. Frontiers in Cellular Neuroscience 11.

Li, Y., Yin, A., Sun, X., Zhang, M., Zhang, J., Wang, P., Xie, R., Li, W., Fan, Z., Zhu, Y., et al. (2017b). Deficiency of tumor suppressor NDRG2 leads to attention deficit and hyperactive behavior. Journal of Clinical Investigation 127, 4270-4284.

Lim, C.S., Kim, H., Yu, N.K., Kang, S.J., Kim, T., Ko, H.G., Lee, J., Yang, J.E., Ryu, H.H., Park, T., et al. (2017). Enhancing inhibitory synaptic function reverses spatial memory deficits in Shank2 mutant mice. Neuropharmacology 112, 104-112.

Loncle, N., Agromayor, M., Martin-Serrano, J., and Williams, D.W. (2015). An ESCRT module is required for neuron pruning. Scientific Reports 5, 8461.

Lund, I.V., Hu, Y., Raol, Y.H., Benham, R.S., Faris, R., Russek, S.J., and Brooks-Kayal, A.R. (2008). BDNF selectively regulates GABAA receptor transcription by activation of the JAK/STAT pathway. Science Signaling 1.

Morris, R.G.M., Garrud, P., Rawlins, J.N.P., and O'Keefe, J. (1982). Place navigation impaired in rats with hippocampal lesions. Nature 297, 681-683.

Moy, S.S., Nadler, J.J., Perez, A., Barbaro, R.P., Johns, J.M., Magnuson, T.R., Piven, J., and Crawley, J.N. (2004). Sociability and preference for social novelty in five inbred strains: An approach to assess autistic-like behavior in mice. Genes, Brain and Behavior 3, 287-302.

Naaijen, J., Bralten, J., Poelmans, G., Glennon, J.C., Franke, B., Buitelaar, J.K., Faraone, S., Asherson, P., Banaschewski, T., Buitelaar, J., et al. (2017). Glutamatergic and GABAergic gene sets in attention-deficit/hyperactivity disorder: Association to overlapping traits in ADHD and

autism. Translational Psychiatry 7.

Neale, B.M., Medland, S.E., Ripke, S., Asherson, P., Franke, B., Lesch, K.P., Faraone, S.V., Nguyen, T.T., Schäfer, H., Holmans, P., et al. (2010). Meta-analysis of genome-wide association studies of attention-deficit/ hyperactivity disorder. Journal of the American Academy of Child and Adolescent Psychiatry 49, 884-897.

Nicolas, C., Peineau, S., Amici, M., Csaba, Z., Fafouri, A., Javalet, C., Collett, V., Hildebrandt, L., Seaton, G., Choi, S.L., et al. (2012). The JAK/STAT Pathway Is Involved in Synaptic Plasticity. Neuron 73, 374-390.

Oblak, A.L., Rosene, D.L., Kemper, T.L., Bauman, M.L., and Blatt, G.J. (2011). Altered posterior cingulate cortical cyctoarchitecture, but normal density of neurons and interneurons in the posterior cingulate cortex and fusiform gyrus in autism. Autism Research 4, 200-211.

Olton, D.S., and Paras, B.C. (1979). Spatial memory and hippocampal function. Neuropsychologia 17, 669-682.

Peça, J., Feliciano, C., Ting, J.T., Wang, W., Wells, M.F., Venkatraman, T.N., Lascola, C.D., Fu, Z., and Feng, G. (2011). Shank3 mutant mice display autistic-like behaviours and striatal dysfunction. Nature 472, 437-442.

Peñagarikano, O., Abrahams, B.S., Herman, E.I., Winden, K.D., Gdalyahu, A., Dong, H., Sonnenblick, L.I., Gruver, R., Almajano, J., Bragin, A., et al. (2011). Absence of CNTNAP2 leads to epilepsy, neuronal migration abnormalities, and core autism-related deficits. Cell 147, 235-246.

Petsalaki, E., Dandoulaki, M., and Zachos, G. (2018). Chmp4c is required for stable kinetochore-microtubule attachments. Chromosoma 127, 461-473.

Plessen, K.J., Bansal, R., Zhu, H., Whiteman, R., Amat, J., Quackenbush, G.A., Martin, L., Durkin, K., Blair, C., Royal, J., et al. (2006). Hippocampus and amygdala morphology in attention-deficit/hyperactivity disorder. Archives of General Psychiatry 63, 795-807.

Punja, S., Shamseer, L., Hartling, L., Urichuk, L., Vandermeer, B., Nikles, J., and Vohra, S. (2016). Amphetamines for attention deficit hyperactivity disorder (ADHD) in children and adolescents. Cochrane Database of Systematic Reviews 2016.

Robertson, C.E., Ratai, E.M., and Kanwisher, N. (2016). Reduced GABAergic Action in the Autistic Brain. Current Biology 26, 80-85.

Rosciglione, S., Thériault, C., Boily, M.O., Paquette, M., and Lavoie, C. (2014). GÎ± s regulates the post-endocytic sorting of G protein-coupled receptors. Nature Communications 5.

Schmeisser, M.J., Ey, E., Wegener, S., Bockmann, J., Stempel, A.V., Kuebler, A., Janssen, A.L., Udvardi, P.T., Shiban, E., Spilker, C., et al. (2012). Autistic-like behaviours and hyperactivity in mice lacking ProSAP1/Shank2. Nature 486, 256-260.

Schneider, T., and Przewłocki, R. (2005). Behavioral alterations in rats prenatally to valproic acid: Animal model of autism. Neuropsychopharmacology 30, 80-89.

Schoch, H., Kreibich, A.S., Ferri, S.L., White, R.S., Bohorquez, D., Banerjee, A., Port, R.G., Dow, H.C., Cordero, L., Pallathra, A.A., et al. (2017). Sociability Deficits and Altered Amygdala Circuits in Mice Lacking Pcdh10, an Autism Associated Gene. Biological Psychiatry 81, 193-202.

Schuh, A.L., and Audhya, A. (2014). The ESCRT machinery: From the plasma membrane to endosomes and back again. Critical Reviews in Biochemistry and Molecular Biology 49, 242-261.

Scoles, H.A., Urraca, N., Chadwick, S.W., Reiter, L.T., and Lasalle, J.M. (2011). Increased copy number for methylated maternal 15q duplications leads to changes in gene and protein expression in human cortical samples. Molecular Autism 2.

Selimbeyoglu, A., Kim, C.K., Inoue, M., Lee, S.Y., Hong, A.S.O., Kauvar, I., Ramakrishnan, C., Fenno, L.E., Davidson, T.J., Wright, M., et al. (2017). Modulation of prefrontal cortex excitation/inhibition balance rescues social behavior in CNTNAP2-deficient mice. Science Translational Medicine 9.

Skibinski, G., Parkinson, N.J., Brown, J.M., Chakrabarti, L., Lloyd, S.L., Hummerich, H., Nielsen, J.E., Hodges, J.R., Spillantini, M.G., Thusgaard, T., et al. (2005). Mutations in the endosomal ESCRTIII-complex subunit CHMP2B in frontotemporal dementia. Nature Genetics 37, 806-808.

Sweeney, N.T., Brenman, J.E., Jan, Y.N., and Gao, F.B. (2006). The Coiled-Coil Protein Shrub Controls Neuronal Morphogenesis in Drosophila. Current Biology 16, 1006-1011.

Tabuchi, K., Blundell, J., Etherton, M.R., Hammer, R.E., Liu, X., Powell, C.M., and Südhof, T.C. (2007). A neuroligin-3 mutation implicated in autism increases inhibitory synaptic transmission in mice. Science 318, 71-76.

The Dutch-Belgian Fragile, X.C., Bakker, C.E., Verheij, C., Willemsen, R., van der Helm, R., Oerlemans, F., Vermey, M., Bygrave, A., Hoogeveen, A., Oostra, B.A., et al. (1994). Fmr1 knockout mice: A model to study fragile X mental retardation. Cell 78, 23-33.

Tsien, J.Z., Huerta, P.T., and Tonegawa, S. (1996). The essential role of hippocampal CA1 NMDA receptor-dependent synaptic plasticity in spatial memory. Cell 87, 1327-1338.

Vorhees, C.V., and Williams, M.T. (2006). Morris water maze: Procedures for assessing spatial and related forms of learning and memory. Nature Protocols 1, 848-858.

Wang, X., McCoy, P.A., Rodriguiz, R.M., Pan, Y., Je, H.S., Roberts, A.C., Kim, C.J., Berrios, J., Colvin, J.S., Bousquet-Moore, D., et al. (2011). Synaptic dysfunction and abnormal behaviors in mice lacking major isoforms of Shank3. Human Molecular Genetics 20, 3093-3108.

Won, H., Lee, H.R., Gee, H.Y., Mah, W., Kim, J.I., Lee, J., Ha, S., Chung, C., Jung, E.S., Cho, Y.S., et al. (2012). Autistic-like social behaviour in Shank2-mutant mice improved by restoring NMDA receptor function. Nature 486, 261-265.

Yabuki, Y., Shioda, N., Maeda, T., Hiraide, S., Togashi, H., and Fukunaga, K. (2014). Aberrant CaMKII activity in the medial prefrontal cortex is associated with cognitive dysfunction in ADHD model rats. Brain Research 1557, 90-100.

Yamaguchi, H., Aiba, A., Nakamura, K., Nakao, K., Sakagami, H., Goto, K., Kondo, H., and Katsuki, M. (1996). Dopamine D2 receptor plays a critical role in cell proliferation and proopiomelanocortin expression in the pituitary. Genes to Cells 1, 253-268.

Yang, P., Cai, G., Cai, Y., Fei, J., and Liu, G. (2013). Gamma aminobutyric acid transporter subtype 1 gene knockout mice: A new model for attention deficit/hyperactivity disorder. Acta Biochimica et Biophysica Sinica 45, 578-585.

Yizhar, O., Fenno, L.E., Prigge, M., Schneider, F., Davidson, T.J., Ogshea, D.J., Sohal, V.S., Goshen, I., Finkelstein, J., Paz, J.T., et al. (2011). Neocortical excitation/inhibition balance in information processing and social dysfunction. Nature 477, 171-178.

Yue, F., Cheng, Y., Breschi, A., Vierstra, J., Wu, W., Ryba, T., Sandstrom, R., Ma, Z., Davis, C., Pope, B.D., et al. (2014). A comparative encyclopedia of DNA elements in the mouse genome. Nature 515, 355-364.

Zablotsky, B., Black, L.I., Maenner, M.J., Schieve, L.A., and Blumberg, S.J. (2015). Estimated prevalence of autism and other developmental disabilities following questionnaire changes in the 2014 national health interview survey. In National Health Statistics Reports.

Zhou, Y., Kaiser, T., Monteiro, P., Zhang, X., Van der Goes, M.S., Wang, D., Barak, B., Zeng, M., Li, C., Lu, C., et al. (2016). Mice with Shank3 Mutations Associated with ASD and Schizophrenia Display Both Shared and Distinct Defects. Neuron 89, 147-162.

국문 초록

'정신 장애 진단 및 통계 편람' 5판 (DSM-5)에 따르면, 신경발달장애는 우리 일생에 있어 상대적으로 이른 시기에 진행되는 발달과정에서 나타나는 어떠한 문제로 인해 학습과 기억, 운동력, 주의력, 사회성 등 행동 및 인지적 기능의 장애를 유래하게 되는 상태를 말한다.

이러한 신경발달장애는 지적장애, 자폐 범주성 장애 (ASD), 주의력 결핍 과잉행동 장애 (ADHD), 강박장애, 틱장애 등 그 행동 및 정신적 증상에 따라 다양하게 세분화 되며, 많은 경우에 이러한 장애를 가진 환자들 사이에서 비슷한 증상들이 나타나곤 한다. 그러나 각각의 장애의 원인과 메커니즘에 대해서는 아직 잘 알려져 있지 않으며, 하나의 장애라고 할지라도 서로 다른 다양한 메커니즘이 관여하는 것으로 보인다.

신경발달장애중에 자폐 범주성 장애는 사회성과 사회적 의사소통의 문제, 반복적인 행동과 제한적인 관심사로 특정된다. 이러한 자폐 범주성 장애는 전세계적으로 유병률 이 높아 다양한 유전적 연구들이 이루어지고 있으며 SH3 and multiple ankyrin repeat domains protein 2 (*SHANK2*) 유전자는 자폐 범주성 장애와 관련이 있는 유전자 중 하나로 알려져 있다. 실제로 각각 엑손 6/7번과 7번이 제거된 (*Shank2* KO e67과 *Shank2* KO e7), 두 종류의 *Shank2* 유전자 결손 생쥐가 자폐 행동을 보이는 것이 보고 되었다. 나는 이 두 생쥐로 전사체 분석을 진행하였고 흥미롭게도 *Shank2* KO e67 생 쥐에서만 ɣ-aminobutyric acid (GABA) A 수용체의 섭유닛 α2 (GABAAα2)를 인코딩하 는 *Gabra2*라는 유전자의 발현이 줄어들고 이로 인해 억제성 신경전달이 감소하는 것 을 발견했다. 이 때 흥분성 신경전달은 정상적이었으며, 따라서 흥분성과 억제성 신경 전달의 균형 (E/I balance)가 망가졌다고 볼 수 있다. 나는 감소한 억제성 신경전달을 회복시켜주는 처리를 통해 *Shank2* KO e67 생쥐의 공간 기억 장애가 향상되는 것을 볼 수 있었고, 같은 처리로 인해 *Shank2* KO e7의 장애는 회복되지 않았다.

이와 더불어, endo-lysosomal 메커니즘이 신경발달 과정에 어떠한 영향을 주는지 알아보았다. 흥미롭게도 발달 과정상의 뉴런 컬쳐에서, endosomal sorting complexes

required for transport III (ESCRT‑ III)를 이루는 *Snf7‑3*라는 단백질의 발현을 감소시키자 뉴런의 수상돌기들이 증가하는 것을 볼 수 있었다. 나는 이러한 현상이 신경발달 장애의 증상들과 관련이 있는지 알아보기 위해 *Snf7‑3* 유전자가 모든 세포에서 결손되거나, 뇌의 흥분성 뉴런에서만 결손 되는 두 종류의 생쥐를 만들었고, 이 마우스들은 ADHD의 주요 증상 중 하나인 hyperactivity를 나타냈다. 뿐만 아니라 후자의 생쥐의 경우 물체의 위치에 대한 기억이 손상되는 것을 볼 수 있었다. 추가로 E/I balance가 많은 신경발달 장애 모델 생쥐에서 손상되어 있기 때문에, 이를 *Snf7‑3* 결손 생쥐에서도 살펴보았으며, 자동적으로 발생하는 흥분성 신경전달 빈도가 이 결손 생쥐들에서 증가해 있는 것을 확인할 수 있었다.